PHYSICAL REVIEW
LETTERS

VOLUME 5 JULY 15, 1960 NUMBER 2

STEADY COMPONENT OF THE INTERPLANETARY MAGNETIC FIELD: PIONEER V*

P. J. Coleman, Jr., Leverett Davis, † and C. P. Sonett
Space Technology Laboratories, Incorporated, Los Angeles, California
(Received June 22, 1960)

The purpose of this Letter is to report some of the observations made with the magnetometer carried aboard Pioneer V. We have examined the data for the first 50 days of operation. These data include measurements in the distant field of the earth, the geomagnetic boundary, and interplanetary space. However, the subject of this note concerns only the latter observations and, specifically, an apparent steady component of the interplanetary magnetic field.

The equipment used for this experiment was similar to the search coil magnetometer carried on both Pioneer I[1] and Explorer VI;[2,3] it measured $B_{\perp}$, the magnitude of the component of the magnetic field normal to the spin axis of the vehicle. Some circuit modifications have been made, principally to decrease the amplifier threshold to 0.1 gamma (1 gamma $\equiv 10^{-5}$ gauss). The details of the equipment have been published elsewhere.[4] A major contribution to magnetic noise in the vehicle was expected to be solar cell current ripple, produced by the variation of the solar cell illumination as the vehicle rotated. Since no effect due to this cause could be detected as the angle of illumination changed considerably, this effect must be negligible. Dessler[5] has suggested, as another possible source of error, that the permanent field of the vehicle would be affected by a solar wind so as to produce a field modulated at the spin rate. A partial investigation of this effect indicates that it is unlikely to be significant. The minimum observed field values have been 0.35 gamma, which provide an upper bound on the threshold of the instrument. Higher values of the field ranging from 5 to over 60 gammas were observed when geomagnetic storms occured on earth. The observed field has decreased to below 1 gamma on two occasions separated by a 27-day period. Thus, these low readings, and in particular those of the order of 2.7 gammas, which are of primary concern here, appear to be valid measurements rather than artifacts or noise.

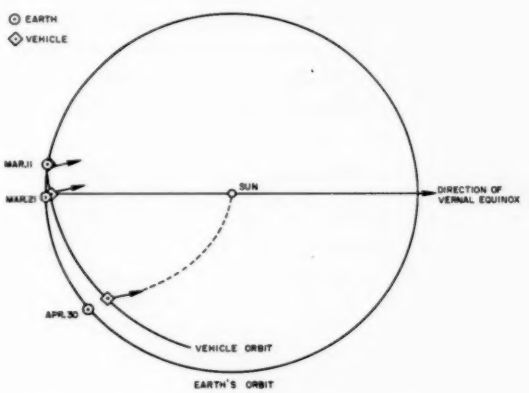

FIG. 1. Ecliptic plane view of Pioneer V orbit. The dashed line represents a typical field line based upon Parker's model. The arrows show the direction of the spin axis when projected into the ecliptic plane.

The Pioneer V vehicle was launched at 1300 GMT on March 11, 1960, during the recovery phase of a magnetic storm. The orbit of the vehicle is an ellipse of aphelion 1.5×10^{8} km and perihelion 1.2×10^{8} km, designed to approximately intersect the Venusian orbit on August 9, 1960. The vehicle was spin-stabilized at approximately 2.5 rps, so that, as shown in Fig. 1, the orien-

Copyright 1960 by the
American Physical Society

tation of its spin axis is invariant in an inertial coordinate system. The angle between the spin axis of the vehicle and the radius to the sun decreased from 27° on March 11 to 2° on April 8, and then increased to 22° on April 30. During this interval, the sun rotated 1.9 times as seen from the earth, the vehicle and the earth moved 50° around the sun (approximately 12×10^7 km), and the vehicle decreased its distance from the sun by 7.5×10^6 km or five percent.

Values of $B_\perp$ observed in this region are plotted in Fig. 2. Measurements were usually transmitted five times daily for periods of approximately 20 minutes. The output of the magnetometer is converted from analog to digital data by the telemetry unit. The shaded area in Fig. 2(a) indicates the maximum range of values of $B_\perp$ corresponding to the range of digital data observed during each transmission. Figure 2(a) indicates the average value observed during each transmission. From the figure, it is apparent that whenever conditions are magnetically stable, as on March 13, 18, 22 and April 9, 17, 18, the observed average value of $B_\perp$ is very nearly 2.7 gammas. On many more days with moderate disturbances, the average field is about this value.

These observations are inconsistent with many models of the interplanetary field, including the usual tacit assumption that the field is essentially zero. A field-free cavity from which the interstellar magnetic field has been swept by the solar wind is excluded[6] also. If the field were imbedded in clouds of turbulent gas emitted from the sun, the measurements would be much more irregular. Even if there were a tendency for the imbedded fields to have some regular pattern, e. g., to be toroidal, not all clouds would be expected to have the same strength, and the orientations would be sufficiently varied to produce noticeable variations in $B_\perp$. A magnetic field swept out radially or along slightly curved beams of solar particles, as suggested by Parker,[7] would yield $B_\perp$ nearly zero when the spin axis is nearly parallel to the beam shown in Fig. 1, and

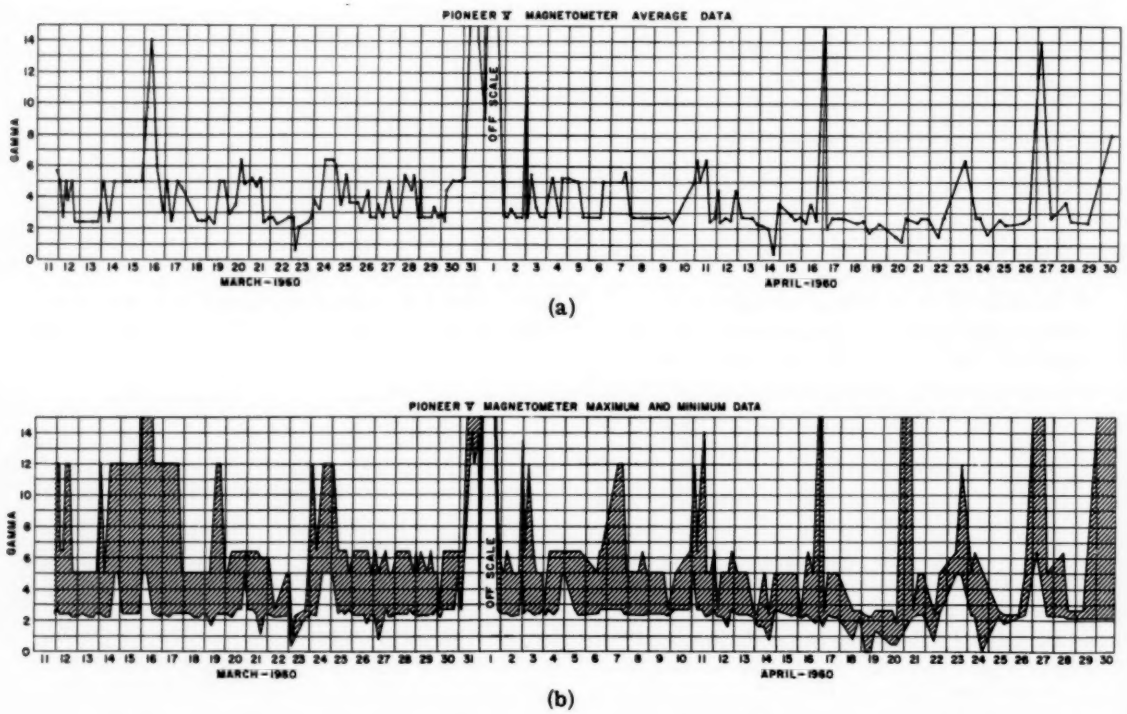

FIG. 2. Pioneer V magnetometer data. (a) (Upper plot) Values of $B_\perp$ averaged over period of data transmission. The points indicate approximate times measurements were made. (b) (Lower plot) Maximum range of $B_\perp$ during transmission. Telemetry data are derived from an analog instrument output and are converted to digital data. The digital transitions in the analog-to-digital converter which are pertinent to this discussion occur at the following values of $B_\perp$ (in gammas): 2.25, 2.35, 2.40, 2.70, and 5.00.

$B_\perp$ would be at least 40% of the total field at either the beginning or the end of the interval considered. Tubes of force originating on regions of the solar surface would contain field strengths varying over a wide range of values and having both polarities. Thus, $B_\perp$ at the vehicle should vary by factors of two or more from week to week. If such a field were wound until it was nearly azimuthal, variations in the angle between the field and spin axis would change $B_\perp$ by only 15%, which might escape observation. However, it would not be expected that, in this case, the total field would be nearly as stable and uniform as the observed field.

The observations suggest that, at this stage of the solar cycle, the interplanetary magnetic field, when undisturbed, is nearly constant in magnitude and nearly uniform in direction over the region explored so far. It seems that the only plausible models exhibiting such properties are a galactic interstellar field that is uniform over the solar system, and a large scale, regular (presumably approximately dipole) field associated with the sun. The axis of the vehicle has right ascension, 1 hr, and declination, 4°. If the interstellar magnetic field were aligned along the spiral arms of the galaxy,[8-10] it would have, approximately, a right ascension, 20 hr , and declination, 35°, and would make an angle of about 75° with the spin axis at the vehicle. Thus, the galactic field would have to be about 2.7 to 3.2 gammas. This is 3 to 5 times the conventional value for the galactic field, but values this large might be acceptable. With the galactic field running through the inner solar system, it seems impossible to explain the frequent arrival at the earth of solar cosmic rays of energy below 10^{10} ev, unless they are trapped in the magnetic field of a gas cloud which travels from the sun to the earth as a bubble in the galactic field. This possibility seems unlikely in view of the short travel time from the sun (10 minutes on February 23, 1956,[11] 1-3 hours on other occasions).[12] A solar dipole field produced by currents in the sun would require fields throughout the photosphere of the order of 200 gauss. The measurements of Babcock[13] exclude a field of this magnitude.

A suggestion is that the field might originate in a ring current with a radius of 5-20 solar radii in the equatorial plane of the sun. A similar model has been proposed, in connection with an analysis of cosmic rays, by Elliot.[14] With such ring radii, the field at the photosphere could be as little as 0.5 gauss, and a small steady outflow of gas from the sun might largely exclude such a field from the photosphere. A field due to such a ring current would allow solar cosmic rays to reach the earth along magnetic lines of force with only about two or three times the travel time required for straight line travel, but it would make it difficult to understand the impact zone phenomena observed with the February 23, 1956 event. However, the February 23 event occurred during an extensive Forbush decrease, and the interplanetary field might have been greatly modified. The magnetic field due to such a ring current would tend to store solar cosmic rays and to allow them to reach the earth more easily when their source is on the visible side of the sun. Of course, this model, or any model having a large scale, nearly uniform field, must provide satisfactory explanations of the way in which galactic cosmic rays reach the earth, the low-energy cutoff, the mechanism of Forbush decreases, and a host of similar problems. However, until more is known of the way the field due to such a ring current would join the galactic field, of the way the field is connected to the sun, and of the manner in which stored particles would be injected into the field, accelerated, and removed, further speculation is premature. Further, it should be noted that both the galactic and the coronal ring field models face very serious difficulties when confronted by Biermann's work on comet tails[15] and are inconsistent with most current ideas on the nature of the solar wind.

Forthcoming experiments should cast additional light on the serious discrepancies between the implications of these observations and present models of the interplanetary field.

The authors wish to acknowledge helpful discussions with J. A. Simpson and E. N. Parker.

---

*This program was supported by the National Aeronautics and Space Administration.

†Permanent address: California Institute of Technology, Pasadena, California.

[1]C. P. Sonett, D. L. Judge, J. M. Kelso, and A. R. Sims, J. Geophys. Research 64, 941 (1959).

[2]C. P. Sonett, E. J. Smith, and A. R. Sims, First International Space Science Symposium, Nice, France, January, 1960 (to be published).

[3]C. P. Sonett, E. J. Smith, D. L. Judge, and P. J. Coleman, Jr., Phys. Rev. Letters 4, 161 (1960).

[4]D. L. Judge, M. G. McLeod, and A. R. Sims, Rev. Sci. Instr. (to be published).

[5]A. J. Dessler (private communication).

[6]L. Davis, Phys. Rev. 100, 1440 (1955).

[7]E. N. Parker, Plasma Dynamics, edited by F. H.

Clauser (Addison-Wesley Publishing Company Inc., Reading, Massachusetts, 1960), p. 248.
[8]L. Davis, Phys. Rev. 96, 743 (1954).
[9]W. A. Hiltner, Astrophys. J. Suppl. 2, 389 (1956).
[10]A. Behr, Nachr. Akad. Wiss. Göttingen, Math.-physik. Kl., p. 185 (1959).
[11]P. Meyer, E. N. Parker, and J. A. Simpson, Phys. Rev. 104, 768 (1956).
[12]K. A. Anderson, R. Arnoldy, R. Hoffman, L. Peterson, and J. R. Winckler, J. Geophys. Research 64, 1133 (1959).
[13]H. D. Babcock, Astrophys. J. 130, 364 (1959).
[14]H. Elliot, Nature 186, 299 (1960).
[15]L. Biermann, Soc. roy. sci. Liège 13, 291 (1953).

COUPLING OF THE SOLAR WIND AND THE EXOSPHERE*

C. P. Sonett
Space Technology Laboratories, Incorporated, Los Angeles, California
(Received June 22, 1960)

It is generally assumed that a solar wind,[1] consisting of a cool neutral plasma, primarily of hydrogen, is transported past the earth and causes termination of the geomagnetic field. This termination occurs where the pressure of the wind normal to the dipolar field lines is equal and opposite to the magnetostatic pressure. The distance of termination is approximately calculable for the subsolar point which is also the stagnation point for the wind.[2] A primary source of data concerning the kinetic energy density, T_ρ, of the wind has been the study of cometary tails of Type 1. Biermann's latest estimate[3] from this source gives a T_ρ equal to 2×10^{-8} erg/cm^3, placing the stagnation point boundary at $\sim 8R_e$ (R_e = earth radius).

The purpose of this Letter is to point to additional evidence for a solar wind which was obtained as the result of two rocket magnetometer experiments carried out at altitudes greater than $14R_e$ and to suggest a possible resolution of the apparent inconsistency of the boundary distance obtained from these two rocket experiments as compared to the figure based upon comet observations. Pioneer I traversed the distant exosphere generally within 15°, and Pioneer V within 45°, of the earth-sun line. On both flights, a field increase followed by a decrease at a rate greater than r^{-3} was observed in the region beyond $13R_e$.[4,5] These data, in conjunction with the appearance of sharp-crested waves (see Fig. 1) whose amplitudes rapidly diminish be-

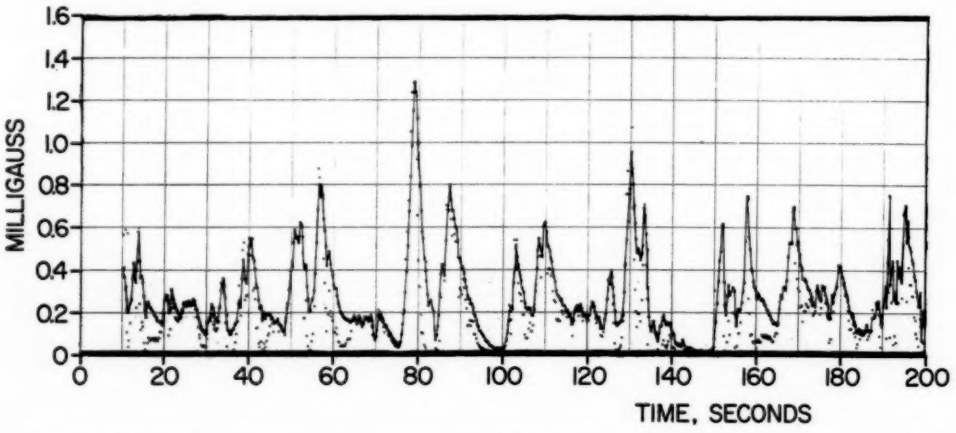

FIG. 1. A typical section of magnetometer data taken in the region of 12 to 13 R_e. The points which are connected with the line are corrected for electronic gain lag in the magnetometer amplifier, whereas the unconnected points are uncorrected. Many of the disturbance pulses shown above have an almost symmetric appearance, indicating little dissipation. The asymmetry of some of the disturbances may be due to pulse pile-up.

yond $14R_e$, bespeak some type of boundary at 13-14 R_e in the region of the stagnation point; this implies a T_ρ of approximately 10^{-10} erg/cm^3 for the incident wind, which is two orders of magnitude smaller than the value from the cometary data. Since these waves appear to exist far into the exosphere ($<7R_e$) with amplitudes comparable to those seen at ~12-14 R_e, considerations of the momentum balance at the geomagnetic boundary should include the forward momentum of these waves. The mean momentum flux of these disturbances at ~$12R_e$ is ~10^{-8} erg/cm^3, including effects of gas pressure in the plasma. Thus, the flux of momentum of these waves is much larger than the solar wind flux, which would produce a boundary at ~$14R_e$. The figure of 10^{-8} erg/cm^3 represents, in fact, a solar wind flux sufficient to compress the geomagnetic field magnetostatically to ~$9R_e$ if we utilize the usual model, or what is equivalent, 10^{-8} erg/cm^3 represents the usual order of magnitude of the value of the solar wind energy density.

The indication from the rocket data of a subsolar boundary at ~13-14 R_e can be made consistent with both the plasma wave momentum flux and the cometary data, provided one invokes a two-step process at the boundary. It is suggested that low-frequency magnetoacoustic waves are generated in a double-stream process between the incoming wind and inelastically stopped gas, that in the lab system (geocentric) only inward propagating waves are of significance, and that these waves carry a considerable fraction of both the momentum and the energy of the incident solar wind deeply into the geomagnetic field without convecting the incident gas body inward.

Clearly, the propagation inward of these disturbances requires that they have a velocity in excess of the characteristic velocities in the medium. For magnetoacoustic disturbances, the modified sonic velocity is 20-30 km/sec, assuming a particle density of $N \sim 10^3$ cm^{-3} and $T \sim 10^4$-10^5 °K. An upper bound for the velocity of the waves of Fig. 1 is 300 km/sec from the expected wind velocity, making them hypersonic. The quasi-symmetry of many of these waves is in partial agreement with the results of the analysis of Davis et al.,[6] though the present data involve the case of looped electron trajectories ($\Delta B/B > 2$). The origin of these waves is clearly in the geomagnetic boundary and does not directly involve astromagnetic fields.

The associated inward transport of energy density is ~0.1 erg/cm^2 - sec in the region of the subsolar (stagnation) point. Dissipation of this energy in a column some $10R_e$ deep requires the radiation of some 10^{-17} watt/cm^3, assuming uniform dissipation with depth. The available loss mechanisms are multistream collective instabilities,[7] bremsstrahlung, synchroton radiation, and Čerenkov radiation, with the latter two probably noncompetitive with the others. It is not possible at the present time to calculate the losses and, therefore, the plasma temperature. It is uncomfortable, however, to require the reradiation of 10^{-17} watt/cm^3, both because of the probable extreme temperature and because of the fact that steady-state radio continuum emissions are not observed from the surface of the earth. Although collective instabilities may cause plasma heating, reradiation is eventually required to maintain an energy balance.

A perhaps more inviting model follows from consideration of the refraction of hydromagnetic waves in the exosphere. A considerable flux of waves will propagate in longitude and perhaps exit on the limbs of the exosphere. Such a mechanism can remove both momentum and energy. Directly on the earth-sun line, propagation will be normally inward upon the atmosphere. Parker[8] has suggested that the generation of standing waves may allow the stopping of forward momentum without an influx of energy for this region of the exosphere.[9] In spite of schemes for removing kinetic energy in order to maintain a reasonable temperature, it is possible that electron temperatures corresponding to tens or hundreds of kilovolts may be established.

The extension of the mechanism suggested in this Letter to storm times is obvious and is presently the subject of investigation. The processes proposed here assume the existence of a solar wind and, therefore, beg the questions raised by the results of Pioneer V, where a field of 2.5 gammas (1 gamma $\equiv 10^{-5}$ gauss) normal to the ecliptic was noted.[10] The author wishes to thank L. Davis, A. J. Dessler, and E. N. Parker for helpful discussions.

---

*Supported by National Aeronautics and Space Administration.

[1]L. Biermann, Soc. roy. sci. Liège 13, 291 (1953).
[2]E. N. Parker, Phys. Fluids 1, 171 (1958).
[3]L. Davis (private communication).
[4]C. P. Sonett, D. L. Judge, A. R. Sims, and J. M. Kelso, J. Geophys. Research 65, 55 (1960).

[5]P. J. Coleman, Jr., C. P. Sonett, D. L. Judge, and E. J. Smith, J. Geophys. Research (to be published).

[6]L. Davis, R. Lüst, and A. Schlüter, Z. Naturforsch. A13, 916 (1958).

[7]See, for example, J. R. Pierce, Proc. Symposium on Physical Processes in the Earth-Sun Environment, Defense Research Telecommunication Establishment, Ottawa, Canada, July 20-21, 1959 (unpublished).

[8]E. N. Parker (private communication).

[9]D. R. Bates, Rocket Exploration of the Upper Atmosphere (Pergamon Press, Ltd., London, 1954), p. 355. It is interesting to note that Bates has computed the required energy input into the lower exosphere as ~ 0.3 erg/cm^2 sec to account for an exospheric temperature of 1500°K.

[10]P. J. Coleman, Jr., L. Davis, and C. P. Sonett, preceding Letter [Phys. Rev. Letters 5, 43 (1960)].

MEASUREMENT OF THE NEUTRON FLUX IN SPACE*

Wilmot N. Hess
Lawrence Radiation Laboratory, University of California, Livermore, California

and

Arthur J. Starnes
Air Force Special Weapons Center, Kirtland Air Force Base, Albuquerque, New Mexico

(Received June 23, 1960)

Neutrons are produced in the atmosphere of the earth by cosmic rays, mostly protons, interacting with oxygen and nitrogen nuclei in the air. About 17% of the neutrons are made at high enough altitude so that they leak out the top of the atmosphere. The flux and energy spectrum of leakage neutrons has been calculated by a multigroup diffusion theory treatment.[1] This leakage of neutrons from the atmosphere should be the principal source of neutrons in space close to the earth.

We have flown a $B^{10}F_3$ neutron detector on an Atlas rocket to an altitude of about 1400 km. This was done in order to check these leakage calculations and to see if there are other important sources of neutrons in space. This detector was used because it can easily distinguish neutrons from other particles.

The detector was mounted on a pod on the outside of the Atlas vehicle and was detached during the flight. The trajectory of the pod is shown in Fig. 1. Also shown here are magnetic latitudes inferred from dip angles. The counts from the BF_3 detector were amplified and discriminated and the counts were telemetered to the ground to several receiving stations.

The trajectory and measured count rate data were combined to give the experimental count rate versus altitude curve shown in Fig. 2. Several interesting features are seen here. The peak in the curve at about 20 km is due to the neutrons in the atmosphere of the earth. The low count rate at higher altitudes is due to neutrons in space. The fact that the neutron flux decreases with altitude outside the atmosphere is in keeping with the thesis that the neutrons counted are from the earth. The increase of counting rate starting at ~1000 km is undoubtedly due to penetration of the Van Allen radiation belt. Protons in the radiation belt when they hit the pod will make neutrons, some of which will be counted, thus causing the increase in the count rate.

The solid curve B shown in Fig. 2 is the calculated counting rate based on the previously calculated neutron leakage, $N(E,\lambda,h)$, from the atmosphere of the earth.[1] The calculated curve

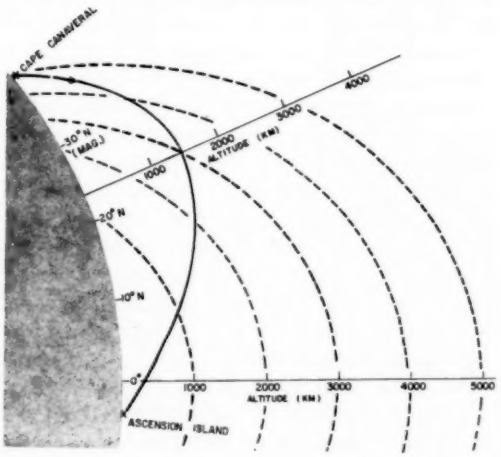

FIG. 1. The approximate trajectory of the Atlas pod flight. Also shown are magnetic latitudes based on dip angles.

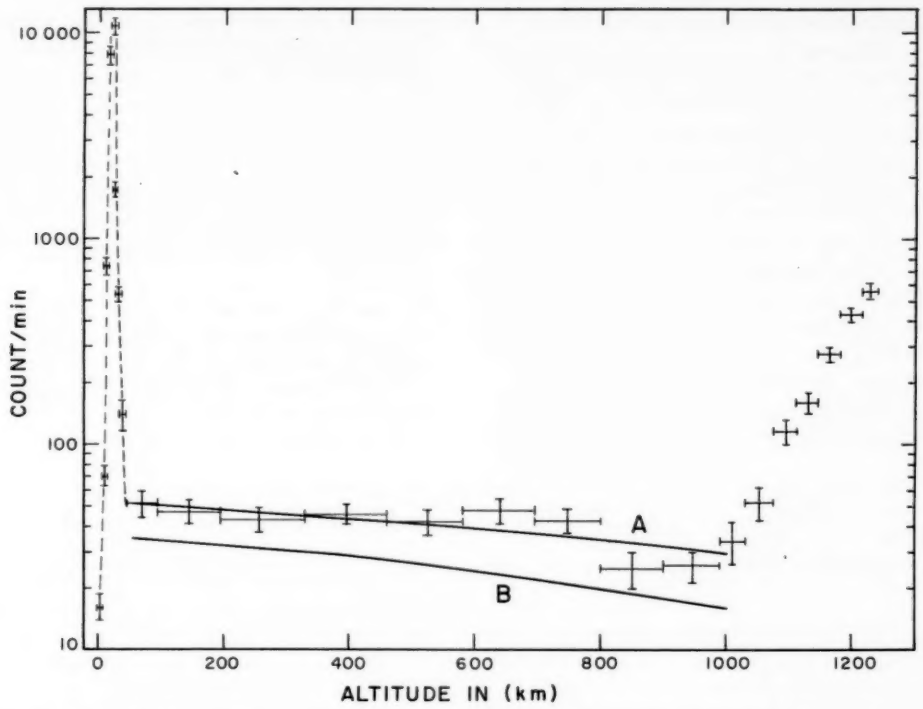

FIG. 2. The neutron detector count rate as a function of altitude. Curve A is a least-squares fit to the experimental data. Curve B is the count rate calculated from earlier work on the neutron leakage flux. No allowance for background counts is made in Curve B.

here includes the change in magnetic latitude of the vehicle (see Fig. 1) as well as the change in altitude. The detector counting rate, C, is calculated by

$$C(h,\lambda)=\int N(E,H,\lambda)\epsilon(E)dE,$$

where h = height from earth surface and λ = geomagnetic latitude. The counter efficiency $\epsilon(E)$ used here is averaged over solid angle. This efficiency was measured by placing Sb-Be, mock fission, and Po-Be neutron sources of known strength at different positions around the counter and measuring the counting rate. The efficiency at 25 kev is 1.15 counts/(neutron/cm^2), at 1 Mev it is 0.65 count/(neutron/cm^2), and at 4 Mev it is 0.35 count/(neutron/cm^2). These measurements are probably accurate to $\pm 20\%$. The leakage spectrum is thought to be good to $\pm 30\%$ so the calculated absolute count rate is probably good to $\pm 35\%$. At 1000 km the calculated rate should be down to 66% of its value at 100 km (for constant λ) because the source is further away. The count rate does not fall off as $1/R^2$ close to the earth as one might think. But due to the angular distribution of the neutrons, it falls off as $1/R^{3.2}$ for the first quarter earth radius. This does not imply a violation of the continuity of flow of particles outwards. The change in magnetic latitude from 100 km altitude to 1000 km should cause a decrease in count rate[2] of 30%. The product of these two effects, a decrease of 53%, is shown in the curve B of Fig. 2.

We have estimated what the detector counting rate from other sources should be. The largest background below the radiation belt will be from cosmic-ray protons producing neutrons in the pod, some of which then will be counted. Calculations of the strength of this background and the measured count rate increase in the radiation belt show that this background should be roughly 0.1 count/sec. The calculated leakage flux[1] at 41°N at the top of the atmosphere is 1.1 neutrons/cm^2 sec which would give in this experiment a

count rate of 0.58 ± 0.20 count/sec. The experimental count rate at 120 ± 70 km is 0.83 ± 0.08 count/sec. Allowing for 0.1 count/sec background these agree well. The calculated count rate decreases from 0.58 to 0.27 at 1000 km and 31°N. A least-squares fit to the experimental data gives a decrease from 0.85 to 0.50 count/sec which agrees quite well with the calculated count rate plus background. We therefore feel that the experimental data on Fig. 2 from 100 km to 1000 km are due mostly to leakage neutrons from the atmosphere of the earth plus a not very well-known background, and the earlier calculations on the neutron leakage are in good agreement with these measurements. This means also that the other sources of neutrons in space near the earth are substantially smaller than the atmospheric leakage source.

Victor Kiernan, Norman Jenson, Donald Peters, and Leonard Gibson of LRL did the electrical engineering of the detection instruments. Nicholas Yanni and Robert Henderson of LRL did the detector mechanical engineering and environmental testing. Captain Alex Kuros and Mr. Olin Long of AFSWC built and tested the telemetering equipment. Also, Major Lew Allen of AFSWC gave his valuable help in carrying out the experiment.

---

*Work was performed under the auspices of the U. S. Atomic Energy Commission.

[1]Hess, Canfield, and Lingenfelter, J. Geophys. Research (to be published).

[2]J. A. Simpson, Phys. Rev. 83, 1175 (1951).

DISLOCATION LOOPS DUE TO QUENCHED-IN POINT DEFECTS IN GRAPHITE

S. Amelinckx and P. Delavignette
Centre d'Etude de l'Energie Nucléaire, Mol, Belgium
(Received June 20, 1960)

Small prismatic dislocation loops, presumably due to the precipitation of vacancies, were first observed in NaCl by means of decoration techniques.[1,2] Unambiguous evidence that, on quenching, dislocation loops are formed in metals (Al, Cu) was presented by Hirsch[3] using transmission electron microscopy. Large dislocation loops due to point defects formed during cold work were found in zinc.[4]

Evidence is presented here that on quenching followed by annealing, dislocation loops are formed in natural graphite, and that the point defects involved are vacancies rather then interstitials.

The graphite crystals were treated in the following way. They were first heated in a vacuum of 10^{-5} mm by means of electron bombardment to around 2700-3000°C for 2 minutes. The electron beam was then switched off suddenly and the crystal flakes were allowed to cool. In about 4 seconds the temperature was below 600°C as judged by pyrometry. After this treatment no change in aspect was found as observed in the electron microscope. After annealing the specimens in a vacuum at 1200°C, it was, however, found that they contained large dislocation loops in the c plane of the kind shown in Fig. 1, which is a transmission electron micrograph of a thin cleavage flake. The loops contain a stacking fault, as can be concluded from the contrast shown in Fig. 1. When using the $(11\bar{2}0)$ reflection to make a dark-field image, it is found that the loop exhibits an inverted line contrast as shown in Fig. 2(b). This observation proves that the Burgers vector is not perpendicular to the c plane. The structure of the dislocation loop is therefore most probably as shown schematically in Fig. 3(a), assuming the point defects to be vacancies. The Burgers vector has a component

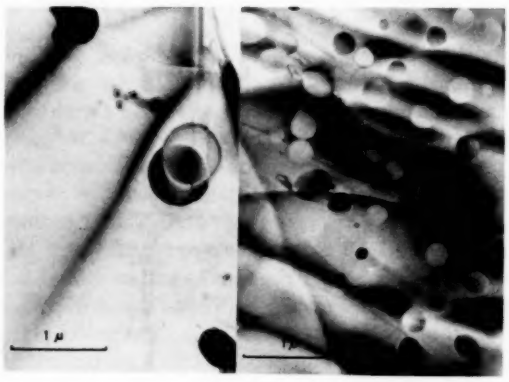

FIG. 1. Quenched-in dislocation loops in graphite. The loops exhibit stacking fault contrast.

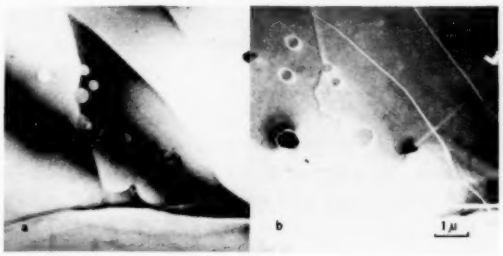

FIG. 2. Normal image (a) and dark-field image (b), using the $(11\bar{2}0)$ reflection. The dislocation line shows up in inverted contrast. This observation eliminates the possibility of a Burgers vector perpendicular to the c plane.

normal to the c plane of $c/2$ and a component in the c plane equal to the nearest neighbor distance. The loop therefore contains a low-energy single stacking fault, i.e., one layer in rhombohedral stacking as shown in Fig. 3(a). This stacking fault cannot be eliminated by glide. Moreover, since the stacking fault energy is very small[5] ($3-5\times10^{-2}$ erg/cm^2), the tendency to do so would be negligible anyhow.

If the point defects were interstitials, the dislocation loops would have the structure of Fig. 3(b). The loop now contains a stacking fault of roughly three times larger energy, since there are three violations of the stacking sequence against one in the first case.

The passage of a partial dislocation with a Burgers vector connecting nearest neighbor carbon atoms could transform this stacking fault into a single one, i.e., of the same type as shown in Fig. 3(a). Since the stacking fault energy γ is so small, the shear stress γ/b is not sufficient to nucleate the partial dislocation and the loop will therefore remain as shown in Fig. 3(b), i.e., with a Burgers vector $\frac{1}{2}c[0,0,0,1]$, i.e., normal to the c plane. Since we find experimentally that the Burgers vector is inclined with respect to the c plane, we have rather strong evidence that the point defects giving rise to the loops are vacancies. We have here an interesting case where the distinction between vacancies and interstitials can be made.

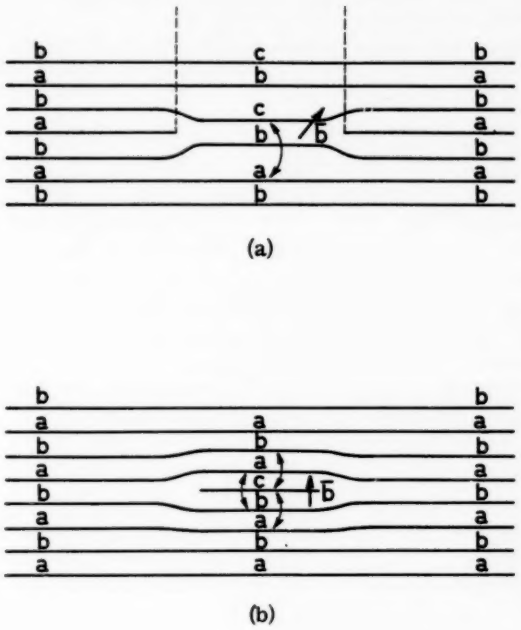

FIG. 3. (a) Schematic view of dislocation loop due to the precipitation of vacancies. The Burgers vector is inclined with respect to the c plane. (b) Schematic view of dislocation loop due to the precipitation of interstitials. The Burgers vector is perpendicular to the c plane.

[1]S. Amelinckx, Lake Placid Conference on Dislocations and Mechanical Properties of Crystals, 1957 (unpublished).

[2]S. Amelinckx, Proceedings of the Raleigh Conference on Mechanical Properties of Engineering Ceramics, 1960 (to be published).

[3]P. B. Hirsch, J. Silcox, R. E. Smallmann, and K. H. Westmacott, Phil. Mag. 3, 897 (1958). P. B. Hirsch and J. Silcox, Proceedings of the Conference on Crystal Growth, Cooperstown, 1958 (unpublished).

[4]A. Fourdeux and A. Berghezan, Compt. rend. 280, 3019 (1960); A. Fourdeux, A. Berghezan, and W. Webb, J. Appl. Phys. (to be published). A. Berghezan, A. Fourdeux, and S. Amelinckx, Acta Met. (to be published).

[5]P. Delavignette and S. Amelinckx, J. Appl. Phys. (to be published).

NUCLEAR MAGNETIC RESONANCE IN SCANDIUM AND LANTHANUM METAL

W. E. Blumberg, J. Eisinger, V. Jaccarino, and B. T. Matthias
Bell Telephone Laboratories, Murray Hill, New Jersey
(Received May 27, 1960)

We have observed the nuclear magnetic resonance (NMR) of Sc^{45} and La^{139} in hexagonal scandium and cubic and hexagonal lanthanum, respectively. The magnitudes of the Knight shift for these d^1 metals, when considered in comparison to the d^3 metals, are found to have an anomalous dependence on the number of d electrons which we suggest results from an enhanced polarization of the s electrons through the s-d exchange interaction. Both these metals exhibit an unexpectedly large temperature dependence of the Knight shift. Measurements were made in the range of temperatures 1.7°K to 300°K in fields extending to 14 koe using a Varian NMR spectrometer. The metals were spectroscopically pure.

The magnitude and temperature dependence of the observed Knight shifts (k) are shown in Fig. 1. The value of k for hexagonal and cubic La is the same at room temperature within the experimental error. Appropriate saturated nitrate solutions were used for establishing the unshifted resonance, at a given field, in each case.

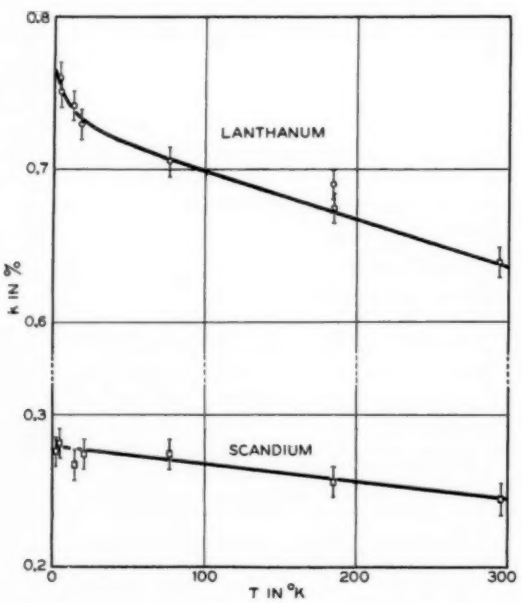

FIG. 1. The Knight shift (k) as a function of temperature for cubic La and hexagonal Sc metals. The indicated errors represent the absolute uncertainties in k, while the relative errors at different temperatures are smaller.

Both line shapes are symmetrical and Gaussian and have widths of 16 oe (Sc) and 13 oe (La) as measured between derivative extrema. The linewidths are independent of temperature and field strength. Although the symmetry of hexagonal Sc allows an electric field gradient, no quadrupole effects were observed. Perhaps this is in part due to the expected smallness of $Q(Sc^{45})$. Strain and self-annealing effects were observed in hexagonal La.

The longitudinal relaxation time (T_1) was measured by observing the degree of saturation as a function of the rf magnetic field strength. In the temperature ranges over which T_1 was measured (1.7°K to 20.2°K for La and 1.7°K to 295°K for Sc), T_1 varied as $1/T$. The product T_1T was 0.2 sec °K for La and 0.6 sec °K for Sc.

At 1.8°K the k for both Sc and La shows an increase of 15% over its value at 295°K. For any reasonable value of thermal expansion coefficients one would predict[1] a change in k of less than $\frac{1}{2}$% of its value in the above temperature range. The temperature dependence of the susceptibility of pure hexagonal La exhibits[2] a paramagnetism that increases with decreasing temperature while Sc, on the other hand, has a temperature-independent Pauli susceptibility.[3] It is worthwhile to point out that a paramagnetic impurity would not produce a temperature-dependent k but would only result in an increasing linewidth with decreasing temperature.[4]

The Knight shift[1] is thought to have its origin in the contact hyperfine interaction between the s conduction electron spin and the magnetic moment of the nucleus in question. Usually the conduction electron polarization is field induced alone via the Pauli susceptibility. For other than d or f group metals the magnitudes of the observed k have been in satisfactory agreement with the simple theory. Until now there has not been a sufficient number of measurements to attempt to correlate the magnitude of k with number of d electrons. In Table I we have arranged k in periodic table form.

As expected, there is an increase in k as one goes from $3d^1$ to $5d^1$ or $3d^3$ to $5d^3$ since the hyperfine interaction increases with Z. How-

Table I. The room temperature values of k for the d^1 and d^3 metals in percent.[a,b]

	d^1	d^2	d^3
$n=3$	$_{21}$Sc: 0.24		$_{23}$V: 0.58
$n=4$			$_{41}$Nb: 0.87
$n=5$	$_{57}$La: 0.63		$_{73}$Ta: 1.1

[a]W. D. Knight, reference 1.
[b]L. H. Bennett and J. I. Budnick, Bull. Am. Phys. Soc. 5, 242 (1960).

ever, the large increase as one proceeds from $3d^1$ to $3d^3$ or $5d^1$ to $5d^3$ is not expected.[5] We suggest that this results from the enhanced s-electron polarization produced by the s-d exchange interaction.

It is noteworthy that the linewidths of Sc, V, Nb, and La are all considerably larger than the direct nuclear dipole-dipole interaction would allow. Since all these elements have single isotopes of overwhelming abundance any indirect exchange interaction would not produce line broadening.[6] The field independence of the linewidth and the line shapes exclude both quadrupolar and anisotropic magnetic contributions. These facts, combined with the Gaussian shape and the temperature independence of the linewidth, indicate a pseudodipolar origin for the observed line shapes.

[1]C. H. Townes, C. Herring, and W. D. Knight, Phys. Rev. 77, 852 (1950), W. D. Knight, Solid State Physics, edited by F. Seitz and D. Turnbull (Academic Press Inc., New York, 1956), Vol II, p. 93.
[2]J. M. Lock, Proc. Phys. Soc. (London) B70, 566 (1957). This author reports a Curie-Weiss behavior with the Curie constant indicating an effective magnetic moment of one-half of a Bohr magneton.
[3]R. M. Bozorth (private communication).
[4]K. Yosida, Phys. Rev. 106, 893 (1957).
[5]One must of course allow for the fact that all of the 4f elements occur between La and Ta.
[6]M. A. Ruderman and C. Kittel, Phys. Rev. 96, 99 (1954).

NUCLEAR MAGNETIC RESONANCE IN α AND β MANGANESE

V. Jaccarino, M. Peter, and J. H. Wernick
Bell Telephone Laboratories, Murray Hill, New Jersey
(Received May 27, 1960)

The properties of the nuclear magnetic resonance (NMR) of Mn^{55} in α and β Mn have been investigated as a function of field and temperature.[1] A very broad asymmetric NMR ($\delta H \sim 250$ oe) was observed in αMn at 295°K. The center of gravity of the resonance corresponds to a negative Knight shift (k) (see Table I). Since there are four magnetically inequivalent sites,[2] it was first thought that the line shape was the result of superposition of several resonances. However, a negligible field dependence was observed for the shape of the line. The α phase is known to have an antiferromagnetic transition at 95°K.[3] Correspondingly, no resonance was visible at 77°K and 20.2°K in the randomly oriented powdered sample.

In βMn only a single resonance line was found, although there occur two physically inequivalent sites. The value of k observed as a function of

Table I. The temperature dependence of the Knight shift in βMn as observed at 14.245 Mc/sec. An error of $\pm 0.02\%$ exists in each of the values given. k was determined with respect to the Mn^{55} NMR in a saturated solution of $LiMnO_4$ and in $KMnO_4$. The field for resonance in the two solutions is identical to one part in 10^5. No chemical shifts have been reported for Mn^{55} in the literature.

T(°K)	k(%)
1.8	-0.11
4.2	-0.11
20.2	-0.12
77	-0.13
190	-0.13
295	-0.13

Table II. The frequency dependence of k and δH for βMn at 295°K. δH is the field separation between points of maximum inflection in the derivative of the line shape. An error of ± 0.02% and ± 1.0 oe is to be assigned to the value of k and δH, respectively.

ν (Mc/sec)	k (%)	δH (oe)
8.000	-0.13	14.6
12.004	-0.14	12.3
14.245	-0.13	11.7

temperature is given in Table I. k is surprisingly both small and negative and, to within the experimental error, temperature independent. At room temperature the line profile is Gaussian. As may be seen in Table II, k is independent of H_0 and δH increases only slightly with decreasing H_0. The intensity of the resonance signal was compared with the NMR signal of niobium metal. From this fact and the inverse field dependence of δH, it appears that all of the Mn atoms contribute to the resonance, and that only the $(1/2 \rightarrow -1/2)$ transition is visible. The change in the width of the resonance line as a function of H_0 which results from the second-order quadrupole interaction indicates that $e^2qQ/h < 1$ Mc/sec.

A monotonically increasing δH with decreasing temperature was observed (see Fig. 1) accompanied by an asymmetry in the line profile at lower temperatures. Saturation effects were observed at 4°K and below. At 20°K, δH is independent of field, indicating that the temperature-dependent contributions to δH are neither of quadrupolar nor of anisotropic magnetic origin.

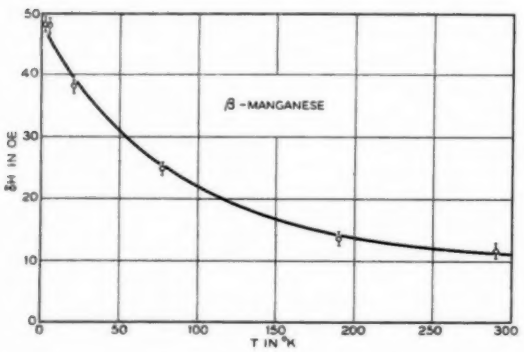

FIG. 1. The linewidth of the NMR of Mn^{55} in βMn as a function of temperature.

The occurrence of an antiferromagnetic transition would produce a similar effect on the NMR signal as was observed in αMn and, hence, such a transition can be ruled out for the β phase above 1.8°K. This result is in agreement with the neutron diffraction measurements of Kasper and Roberts.[4] On the other hand, there is an anomalous contribution to the specific heat[5] at low temperatures which Weiss and Tauer[6] have attributed to a short-range magnetic ordering. It is possible that this ordering is the cause of the increase in linewidth at low temperatures.

Susceptibility measurements have recently been made by Sherwood and Williams (private communication). They find a temperature-independent susceptibility of the order of magnitude of the other nonmagnetic transition metals. This temperature independence is consistent with the temperature behavior of the Knight shift.

In the preceding Letter[7] it was shown that for the d^1 and d^3 metals k is positive. It is interesting to note that not only is k negative for Mn ($3d^5$) and Pt [8] ($5d^8$) but the hyperfine fields in ferromagnetic Fe [9] ($3d^6$) and Co [10] ($3d^7$) are negative as well. While one might hope to explain the negative sign of the hyperfine fields by assuming an exchange polarization[11] of the inner shell s electrons by localized, Hund's rule coupled, d electrons in the case of Fe and Co, it appears that for the other metals such an explanation is unsatisfactory.

The authors are indebted for illuminating discussions, to A. M. Clogston, H. Suhl, and T. Moriya, and wish to thank R. C. Sherwood and H. J. Williams for permission to quote their susceptibility measurements.

[1] Electrolytically deposited, hydrogen-free manganese of 99.9% purity was used in these experiments. αMn (58 atoms per unit cell, symmetry $I\bar{4}3m$) was obtained by annealing for four hours at 625°K. βMn (20 atoms per unit cell, symmetry $P4_132$) was obtained following an annealing period of one hour in argon atmosphere at 850°K, by quenching in ice water. The necessary fine particles were obtained by crushing the metal in a mortar and passing it through a 400-mesh sieve.

[2] W. B. Pearson, Metal Physics and Physical Metallurgy (Pergamon Press, Inc., New York, 1958).

[3] C. G. Shull and M. K. Wilkinson, Revs. Modern Phys. 25, 100 (1953).

[4] J. S. Kasper and B. W. Roberts, Phys. Rev. 101, 537 (1956).

[5] G. L. Booth, F. E. Hoare, and B. T. Murphy, Proc. Phys. Soc. (London) B68, 830 (1955).

[6]R. J. Weiss and K. J. Tauer, J. Phys. Chem. Solids 4, 135 (1958).
[7]W. E. Blumberg, J. Eisinger, V. Jaccarino, and B. T. Matthias, preceding Letter [Phys. Rev. Letters 5, 52 (1960)].
[8]T. J. Rowland, J. Phys. Chem. Solids 7, 95 (1958).
[9]S. S. Hanna, J. Heberle, G. J. Perlow, R. S. Preston, and D. H. Vincent, Phys. Rev. Letters 4, 513 (1960).
[10]A. C. Gossard and A. M. Portis (private communication).
[11]V. Heine, Phys. Rev. 107, 1002 (1957).

MAGNETO-TUNNELING IN InSb

A. R. Calawa, R. H. Rediker, B. Lax, and A. L. McWhorter
Lincoln Laboratory,* Massachusetts Institute of Technology, Lexington, Massachusetts
(Received June 9, 1960)

We have studied the phenomenon of tunneling in InSb at 77°K in magnetic fields up to 88 000 gauss. Current-voltage characteristics with the magnetic field parallel and perpendicular to the current flow across the p-n junction are shown in Figs. 1 and 2. As can be seen from the figures, the effects are comparable for the magnetic field in the two directions. A marked decrease in the tunneling current with increased magnetic field was observed both in forward and reverse bias. The peak voltage is increased by the parallel magnetic field but is not affected to the same extent by the perpendicular magnetic field. A large magnetic effect was also observed in forward bias for the minority carrier injected current.

Several diodes were fabricated by alloying spheres of 99.9% indium and 0.1% cadmium into n-type InSb containing 1.5×10^{17} - 6×10^{17} net impurities per cm^3. Peak to valley current ratios at zero field varied from 1.4 to 1, to 7 to 1 and the diodes showed magneto-tunneling characteristics similar to those shown in Figs. 1 and 2. Measurements have been made with resistors in the magnetic field contiguous to and shunting the diodes so the characteristics in the negative resistance region could be determined as shown. No sensible change in the values of the shunting resistors used was found either with temperature to 77°K or with magnetic field to 88 000 gauss. While the diode of Figs. 1 and 2 was mounted on a Kovar tab, similar results have been obtained for InSb tunnel diodes on nonmagnetic mounts.

The effects of the magnetic field on the tunneling current can be attributed to the creation of magnetic sub-bands and their shift in energy with increasing magnetic field. The rate of Zener tunneling per cm^3 in the absence of a magnetic

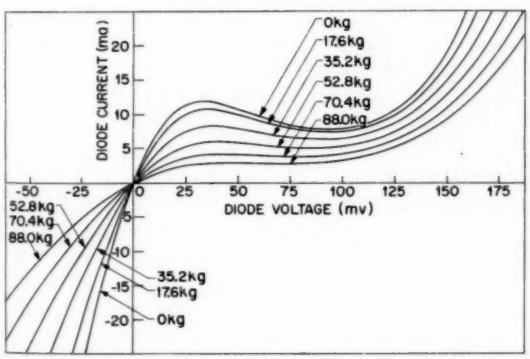

FIG. 1. Current-voltage characteristics at 77°K of an InSb tunnel diode in different magnetic fields parallel to the current flow across the p-n junction. This diode was fabricated using n-type InSb with impurity density $\sim10^{17}$ cm^{-3}.

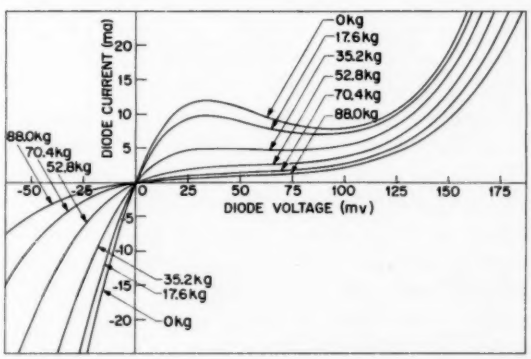

FIG. 2. Current-voltage characteristics at 77°K for the InSb tunnel diode of Fig. 1 in different magnetic fields perpendicular to the current flow across the p-n junction.

field, as given by Kane,[1] is

$$n_0 = C_0 \exp(-\alpha E_g^{3/2}), \quad (1)$$

where $C_0 = F^2 m_r^{1/2}/18\pi\hbar^2 E_g^{1/2}$, $\alpha = \pi m_r^{1/2}/2\hbar F$, F is the force on the electron, m_r is the reduced mass, and E_g is the band gap. In the presence of a magnetic field parallel to the current, Eq. (1) is modified to take into account the tunneling between the magnetic sub-bands of the valence and conduction bands as follows:

$$n_H = C_H \sum_n \exp\{-\alpha[E_g^2 + 4E_g((n+\tfrac{1}{2})\hbar\omega_c \pm \tfrac{1}{2}\mu_B g_0 H)]^{3/4}\}, \quad (2)$$

where $C_H = C_0 \tfrac{3}{2}\alpha E_g^{1/2}$, $\omega_c = eH/m^*c$ is the cyclotron frequency of the electron, μ_B is the Bohr magneton, and g_0 is the g factor. In the derivation of Eq. (2) the nonparabolic nature of the bands in InSb has been taken into account and the equation has been derived on the basis of electron-light hole tunneling[2] where the selection rule $\Delta n = 0$ applies. The g factor, as well as the effective mass, have been taken to be the same for the electron and the light hole ($m^* = 0.013 m_0$, $g = 56$). Assuming that the distance of the Fermi level into both the conduction and valence bands is large compared to the average energy of the tunneling carriers perpendicular to the junction field,[3] Eq. (2) can be approximated to give the result for the normalized current,[4] $I(H)/I(0)$,

$$\frac{I(H)}{HI(0)} \approx A \frac{m}{m^*} \sum_n \exp\left\{-2AH\left[(n+\tfrac{1}{2})\frac{m}{m^*} \pm \frac{g}{4}\right]\right\}, \quad (3a)$$

where

$$A = \frac{3\pi\mu_B m_r^{1/2} E_g^{1/2}}{2\hbar F}; \qquad \mu_B \equiv \frac{e\hbar}{2mc} = \tfrac{1}{2}\frac{\hbar\omega_c}{H}\frac{m}{m^*}.$$

Equation (3a) can be written

$$\frac{I(H)}{HI(0)} = A \frac{m}{m^*} \operatorname{csch}\left(A\frac{m}{m^*}H\right) \cosh\left(\frac{AgH}{2}\right). \quad (3b)$$

The experimental values of $I(H)/HI(0)$ as a function of H for an InSb tunnel diode for four different voltages, two in forward and two in reverse bias in the tunneling region, are plotted in Fig. 3. At sufficiently high magnetic fields only the $n = 0$ sub-bands and negative spin term contribute appreciably to the tunnel current, which allows the one unknown parameter A in Eqs. (3) to be simply determined. The value of A obtained in this way was used to plot the theoretical curve in Fig. 3. Considering the fact that

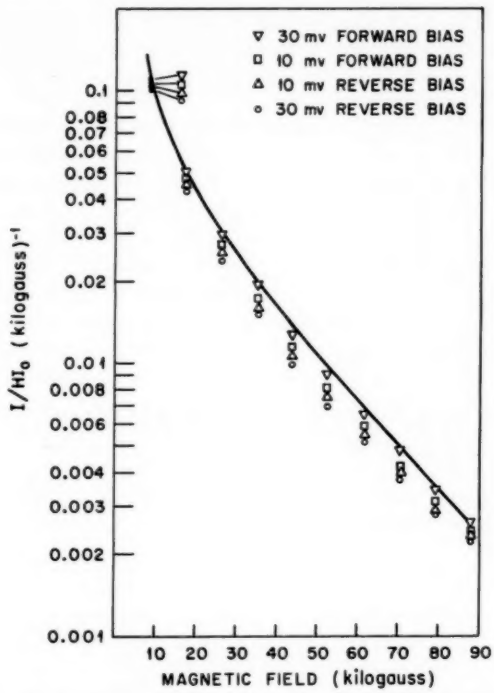

FIG. 3. Points are experimental values of $I(H)/HI(0)$ at 77°K for the diode of Fig. 1 as a function of parallel magnetic field. Values for four different diode voltages in the tunneling region are shown. Also shown is the theoretical curve determined from Eq. (3) with the constant $A = 7.1 \times 10^{-7}$ gauss^{-1}.

A determines both the slope and the absolute value of the curve, the fit is very good. This agreement indicates that the other effects induced by the magnetic field, such as the change in F and the change in the relative position of the Fermi level with respect to the band edges, are of secondary consideration. From the value of $A = 7.1 \times 10^{-7}$ gauss^{-1} one can obtain a value for the field in the junction of 5.4×10^4 volts cm^{-1} for light hole-electron tunneling. Heavy hole-electron tunneling gives a value approximately a factor of $\sqrt{2}$ smaller.

A somewhat more involved theoretical result for the perpendicular case has been obtained using the WKB method. The tunneling is summed over both sets of sub-bands since the selection rules for the magnetic quantum numbers n_1 and n_2 no longer apply.

A magnetic effect of comparable magnitude on the minority carrier current at high forward

biases was also observed in a lightly doped normal diode. A preliminary analysis indicates that the effect is due to the decrease in the number of minority carriers as a result of an effective increase in the gap.

We have also seen a magneto-tunneling effect in Ge confirming the observations of Esaki,[5] but the effect is very small because of the larger masses and the larger electric fields. From the preceding theory low-gap materials would be expected to give the largest effects.

Studies of magneto-tunneling with very high magnetic fields and in crystals with anisotropic energy surfaces should provide information about the energy bands.

The authors wish to thank C. R. Grant for help in taking the data and H. H. Bessler for help in fabricating the diodes. The InSb used was kindly furnished us by A. J. Tuzzolino of Chicago Midway Laboratories and by the materials section of our laboratory. We would like to thank P. Argyres, L. Esaki, and P. Price for discussions on the theoretical aspects of this problem.

---

*Operated with support from the U. S. Army, Navy, and Air Force.

[1]E. O. Kane, J. Phys. Chem. Solids 12, 181 (1959).

[2]This assumption is made by Kane and appears to be consistent with the large magneto-tunneling effect observed. If the tunneling is electron-heavy hole, Eq. (2) must be modified but Eq. (3) is applicable except for a constant factor in A.

[3]J. V. Morgan and E. O. Kane, Phys. Rev. Letters 3, 466 (1959).

[4]A result similar in form to Eq. (3) has been derived by L. Esaki and P. Price (private communication).

[5]L. Esaki (private communication).

OBSERVATION OF STARK SPLITTING OF ENERGY BANDS BY MEANS OF TUNNELLING TRANSITIONS

A. G. Chynoweth, G. H. Wannier, R. A. Logan, and D. E. Thomas
Bell Telephone Laboratories, Murray Hill, New Jersey
(Received June 8, 1960; revised manuscript received June 22, 1960)

It has been shown theoretically[1,2] that the energy states available to an electron in a crystal form a series of Stark ladders if a uniform electric field E is present. The separation of these energy levels is eEd, where d is the spacing of the set of lattice planes perpendicular to the field. One can convince oneself that a structure having this periodicity is present in a given region even if the field E is not homogeneous, but only slowly varying over atomic dimensions. The purpose of this Letter is to present experimental evidence for the occurrence of this predicted structure. This evidence was obtained from studies of the tunnel currents in narrow p-n junctions of indium antimonide.

The junctions were made by alloying pellets of 0.1% Cd in In into n-type InSb crystals. The donor and acceptor concentrations on the n- and p-type sides were 6.7×10^{17} cm^{-3} and 10^{18} cm^{-3}, respectively. The field distribution in the junction was thus fairly symmetric. Using (m^*/m_0) = 0.015 for the electrons and 0.17 for holes, the Fermi energies on the n- and p-type sides were 0.190 ev and 0.022 ev, respectively. These junctions exhibited voltage-current characteristics in which the reverse and forward quadrants were roughly symmetric about the origin, i.e., the junctions were not narrow enough to exhibit Esaki effects.[3] Nevertheless, at all except the very highest forward biases, i.e., >200 mv, the dominant current generation mechanism was tunnelling.[4]

With the junctions immersed in liquid helium, plots of the junction conductance, (dI/dV), against forward bias were obtained by means of automatic conductance plotting equipment. All junctions revealed varying amounts of structure in their conductance plots which could be interpreted in terms of phonon or multiphonon emission processes.[5,6] However, all the junctions with the above impurity concentrations showed additional fine structure at biases lying between 100 and 130 mv. This structure appeared as a small amplitude oscillation of the conductance vs bias curve. Examples of these oscillations are shown in Fig. 1. (The high sensitivity required in order to reveal these oscillations was obtained by a bucking technique. Great care was taken to rule

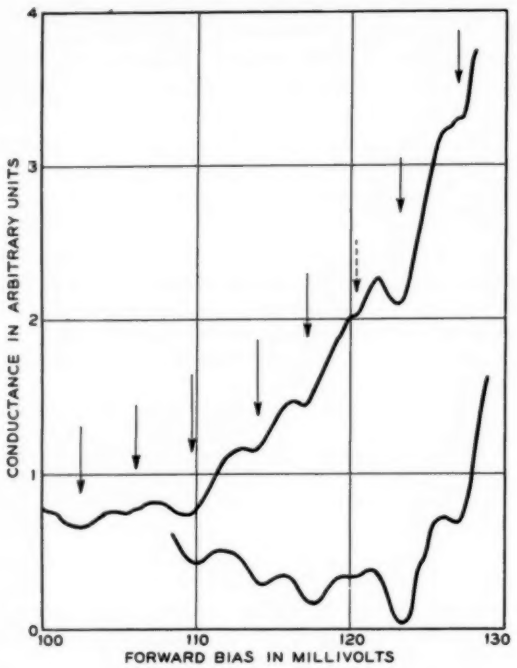

FIG. 1. Plots of conductance (with arbitrary zero) versus forward bias exhibiting Stark oscillations. The two curves were taken using different bucking conditions.

out the possibility that the observed oscillations were caused by cyclic variations in any part of the equipment.) The period of oscillation is almost an order of magnitude too small to be ascribed to multiple emission of optical phonons. It will be shown, on the other hand, that the Stark effect can account for the period of the oscillations as well as the fact that they occur only over a particular range of bias.

To observe the Stark effect it is necessary for the electron to see the same Stark splitting on entering and leaving the tunnel. Referring to Fig. 2, this requires that $E_c = E_v$. Because $V_n \gg V_p$ (the Fermi energies in the n- and p-type sides, respectively), this condition cannot be satisfied until a forward bias of at least V_s is applied to the junction. At this bias, it is possible to equate E_c and E_v at an energy corresponding to the Fermi level on the p-type side. For biases differing appreciably from V_s, matching of Stark levels on the two sides of the junction will be random and independent of bias. As the bias is shifted slightly from V_s, the match in the Stark levels is produced periodically because the two

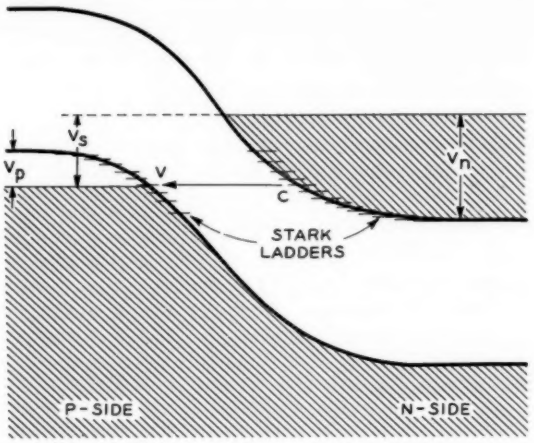

FIG. 2. Diagram defining the symbols used in the text.

sets of Stark levels are swept past each other by the bias. One could also envisage, in principle, a sweep produced by a change in field. This is excluded here because in step junctions, the field E_v at the Fermi level of the valence band is independent of the bias.

If the donor and acceptor concentration and effective masses quoted in the second paragraph are employed for an estimate, it is found theoretically that a forward bias of 105 mv makes E_c and E_v equal. (In making these estimates the distortion to the field distribution caused by the free carrier concentration was taken into account.) This bias is within the range shown in Fig. 2. In the same way one can predict theoretically the common value of this field and hence the magnitude of the Stark splitting. The value found is 2.2 mv. The oscillations of Fig. 2 have a spacing which is about 50% higher. In view of the uncertainties regarding the numbers employed, this is felt to be satisfactory agreement.

The authors are greatly indebted to D. J. Walsh for making the junctions used in this work.

[1]G. H. Wannier, Elements of Solid State Theory (Cambridge University Press, New York, 1959), pp. 190-193.

[2]G. H. Wannier, Phys. Rev. 117, 432 (1960).

[3]L. Esaki, Phys. Rev. 109, 603 (1958).

[4]A. G. Chynoweth and R. A. Logan, Phys. Rev. 118, 1470 (1960).

[5]R. N. Hall, J. H. Racette, and H. Ehrenreich, Phys. Rev. Letters 4, 456 (1960).

[6]H. Holonyak, I. A. Lesk, R. N. Hall, J. J. Tiemann, and H. Ehrenreich, Phys. Rev. Letters 3, 167 (1959).

POSITRON LIFETIME IN METALS

A. Bisi, G. Faini, E. Gatti,* and L. Zappa
Istituto di Fisica del Politecnico, Milano, Italy
(Received May 23, 1960)

The until now available measurements[1-4] of positron lifetime in metals have shown a surprising independence of the electron density. Actually this independence is more apparent than real; the size of the errors quoted in these measurements and the small number of metals investigated do not rule out a variation of lifetime with metals. On the other hand, on the basis of theoretical considerations[5-6] a variation of the annihilation rate with metals is expected; for instance, a 30% variation is predicted between aluminum and sodium.

In the present paper we report the results of our measurements on several metals, which support a dependence of the annihilation rate on the electron density.

Na^{22} was used, which emits positrons accompanied by prompt nuclear γ rays of 1.28-Mev energy. Two plastic scintillators ($1\frac{1}{2}$-inch diam, 1 inch thick), coupled to RCA 6342 photomultipliers, were arranged so that the counters operated by the 1.28-Mev γ rays and by the 0.511-Mev annihilation quanta recorded, respectively, the birth and the death of the positron. The signals were sent into a nanosecond vernier time-delay analyzer[7-8] which was set to accept only the pulses belonging to the two Compton edges. The output pulse heights were measured by means of a ten-channel pulse analyzer. The prompt resolution curve obtained with the γ rays of a Co^{60} sample fit a Gaussian curve with a standard deviation of 3.3×10^{-10} sec. The times of flight over known paths of the γ rays from the same sample were used to calibrate the time scale. The active samples were prepared by evaporating one drop of high specific activity $Na^{22}Cl$ in aqueous solution directly on the different metal targets whose thickness was sufficient to stop the beta particles. This procedure avoids the use of the backing foil which was employed in the previously quoted measurements to support the source and which we have found to give rise to an appreciable reduction of the difference of the annihilation rate in metals. This reduction is present even when the backing foil is very thin (for instance a nylon film of 0.1 mg/cm^2).

The positron lifetime for each metal was obtained by means of relative measurements, i.e., by comparing the centroid shift of its delay curve with that of aluminum. The measurements consisted of several 10-minute recording runs alternately for the Al delay curve and for that of the investigated metal; in this way the instrumental drifts were minimized. The absolute lifetime in aluminum was measured by recording the displacement of the centroid of its delay curve relative to the centroid of the prompt resolution curve from Co^{60} obtained under otherwise identical conditions. This displacement was measured about every five runs of the relative measurements and was checked to remain remarkably constant during the whole investigation. The so-obtained positron mean life in Al was

$$\tau_{Al} = (2.57 \pm 0.06) \times 10^{-10} \text{ sec.}$$

This result disagrees with that of Bell and Graham[2] but shows quite satisfactory agreement with the more recent values given by Gerholm[4] and Minton.[3]

All the results obtained are reported in Table I

Table I. The difference, $\Delta\tau$ (in 10^{-10} sec), between the positron mean life in various metals and that in Al; and the annihilation rate, λ (in 10^9 sec^{-1}).

Z	Metal	$\Delta\tau$	λ
4	Be	$+0.138 \pm 0.110$	3.70 ± 0.17
26	Fe	-0.573 ± 0.035	5.02 ± 0.17
28	Ni	-0.607 ± 0.055	5.10 ± 0.21
29	Cu	-0.283 ± 0.055	4.39 ± 0.16
30	Zn	-0.214 ± 0.062	4.25 ± 0.16
42	Mo	-0.704 ± 0.055	5.38 ± 0.23
46	Pd	-0.200 ± 0.062	4.22 ± 0.15
47	Ag	-0.179 ± 0.035	4.18 ± 0.12
48	Cd	-0.173 ± 0.048	4.17 ± 0.13
49	In	$+0.131 \pm 0.090$	3.70 ± 0.14
50	Sn	-0.124 ± 0.048	4.10 ± 0.13
51	Sb	$+0.711 \pm 0.069$	3.05 ± 0.08
73	Ta	-0.400 ± 0.048	4.61 ± 0.16
74	W	-0.373 ± 0.035	4.56 ± 0.14
78	Pt	-0.587 ± 0.062	5.05 ± 0.22
79	Au	-0.311 ± 0.055	4.43 ± 0.16
82	Pb	$+0.097 \pm 0.048$	3.76 ± 0.11
83	Bi	$+0.297 \pm 0.027$	3.50 ± 0.08

where the annihilation rates and the differences between the positron lifetime in the various metals and that in Al are collected. The quoted errors represent the experimental standard deviation of the mean values.

It is apparent that the difference between the positron lifetimes in various metals and that in Al amounts to ± 35%. It is perhaps interesting to note that the greater lifetimes pertain to those metals for which the angular distribution of annihilation radiation is sharper and can be nearly accounted for by the Fermi theory of the metal electrons.[9-10]

An attempt to correlate the annihilation rate with the electron density is shown in Fig. 1,

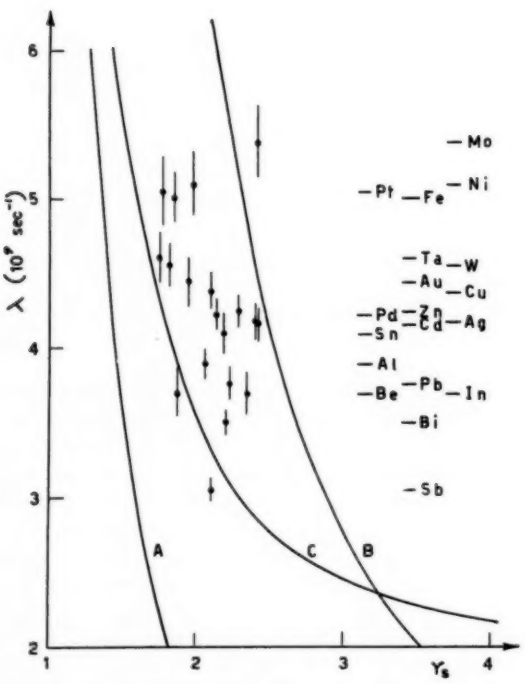

FIG. 1. Positron annihilation rate in metals as a function of the radius of the unit electron sphere. *A*, *B*, and *C* are theoretical curves (see text).

where the various metals are distinguished only by the dimensionless quantity r_s defined as the radius of the so-called unit electron sphere[5]:

$$r_s = 1.384(A/\rho z)^{\frac{1}{3}};$$

z, ρ, and A are the valence, density, and atomic weight. We have chosen the z values on the basis of the more important oxidation states. An approximate correction was introduced in order to allow for the fact that the volume accessible to free electrons is limited by the size of the ionic volume; obviously this correction is important only for the noble metals where the cores nearly touch each other. In the same figure three theoretical curves labelled *A*, *B*, and *C* are reported. The first is calculated according to the Sommerfeld free electron theory; the second, due to Ferrell,[5] takes into account that the actual electron density at the positron is greater than the average because of the Coulomb interaction between positron and electrons. Finally the curve *C* is calculated according to the alternative suggested by Gerholm[4] on the assumption of positronium formation.

---

*Istituto di Fisica del Politecnico and Laboratori CISE, Milano, Italy.

[1]S. DeBenedetti and H. J. Richings, Phys. Rev. 85, 377 (1952).

[2]R. E. Bell and R. L. Graham, Phys. Rev. 90, 634 (1953).

[3]G. E. Minton, Phys. Rev. 94, 758 (1954).

[4]T. R. Gerholm, Arkiv Fysik 10, 523 (1956).

[5]R. A. Ferrell, Revs. Modern Phys. 28, 308 (1956).

[6]S. Kahana, Phys. Rev. 117, 123 (1960).

[7]C. Cottini, E. Gatti, V. Svelto, and F. Vaghi, Proceedings of the Second Symposium on Advances in Fast Pulse Techniques for Nuclear Counting, Lawrence Radiation Laboratory, Berkeley, February, 1959 (unpublished).

[8]E. Gatti and V. Svelto, Nuclear Instr. 4, 189 (1959).

[9]G. Lang, S. DeBenedetti, and R. Smoluchowski, Phys. Rev. 99, 596 (1955).

[10]A. T. Stewart, Can. J. Phys. 35, 168 (1957).

OBSERVATION OF THE "ISOTOPE EFFECT" IN THE NUCLEAR CAPTURE OF NEGATIVE MUONS BY CHLORINE*†

W. J. Bertram, Jr.,‡ R. A. Reiter, T. A. Romanowski, and R. B. Sutton
Carnegie Institute of Technology, Pittsburgh, Pennsylvania
(Received June 24, 1960)

Theoretical calculations by various authors[1-3] of the muon capture rates in nuclei have shown that a strong "isotope effect" is to be expected. Primakoff,[1] using a closure approximation, has found that

$$\lambda_c(a) = (Z_{\text{eff}})^4(\langle\eta\rangle_a)^2(272\ \text{sec}^{-1})\left(1 - \frac{A-Z}{2A}\,\delta_a\right),$$

where $\delta_a = 3.0$. This formula predicts a quite large isotope effect, e.g., $\lambda_c(Cl^{37})/\lambda_c(Cl^{35}) = 0.83$. Primakoff's calculations are intended to give an idea of the general behavior of the capture rate over all ranges of Z and A, and do not predict the exact value for any particular nucleus. In fact, δ_a is only independent of Z and A in the first approximation.

Tolhoek and Luyten,[2] using the shell model of the nucleus, have explicitly evaluated the transition probabilities between the various nuclear energy levels, and performed the summation appropriate to each nucleus.

We have measured the "isotope effect" in separated chlorine isotopes using the physical arrangement shown in Fig. 1. The composition of the beam from the CIT synchrocyclotron was about 70% muons, and 30% electrons, with a negligible amount of pions. The lead wall collimated the beam to a size $1\frac{1}{2}$ in. × $1\frac{1}{2}$ in., and

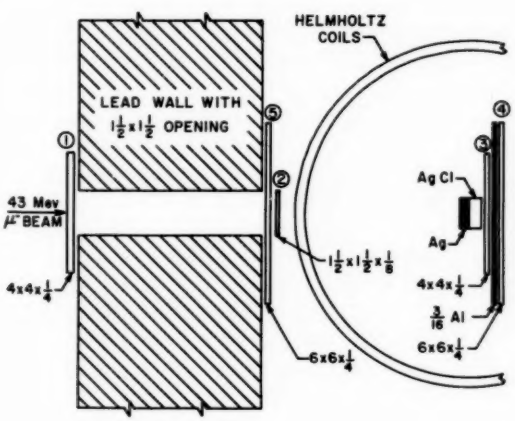

FIG. 1. Experimental arrangement.

helped to reduce the random counting rate in the electron telescope. The Helmholtz coils were adjusted to buck out the fringing field of the cyclotron. This eliminated the sinusoidal modulation of the decay curve due to precession of the muon spin about the field direction.

The targets used consisted of enriched isotopes of chlorine in the form of AgCl. They were 1-inch diameter cylinders of length 1/4 in. and 5/8 in., respectively, for the Cl^{37} and the Cl^{35} isotopes. The enriched abundances were 76% Cl^{37} and 96.8% Cl^{35}. An amount of silver absorber, sufficient to maximize the number of stopped muons, was placed directly in front of the target.

A muon which stopped in the target was indicated by a coincidence $(1+2+\bar{3})$, where the bar indicates that the counter is in anticoincidence. The lack of a monitor directly in front of the target did not appreciably increase the random background, but did significantly reduce the background arising from muons which would stop in such a counter. A decay electron was indicated by a coincidence $(3+4+\bar{5})$. Counter 5, in anticoincidence, prevented particles which came through the collimator from being counted as electrons. In order to reduce the random background arising from gamma rays and neutrons, 3/16 in. of aluminum was placed between counters 3 and 4.

The "start" pulses $(1+2+\bar{3})$ opened a fast rising gate, which was closed by the "stop" pulses $(3+4+\bar{5})$. If no electron was detected within 15 μsec, the gate was closed by the delayed "start" pulses. The pulses from a precision 10-Mc/sec oscillator passed through the gate and were counted by a 10-Mc/sec scaler. After 15 microseconds the number of counts in the 10-Mc/sec scaler, corresponding to the time difference between "start" and "stop" pulses, was stored in the memory of an RCL 256-channel pulse-height analyzer.

The data from the time analyzer form a histogram which is fitted by

$$Y_n = e^{-n\lambda_b}\left[Ae^{-n\lambda_t(\text{Ag})} + B\left(\alpha_{35}e^{-n\lambda_t(35)} + \alpha_{37}e^{-n\lambda_t(37)}\right) + Ce^{-n\lambda_t(\text{C})} + D\right],$$

where A, B, C, D are constants, and n is an integer corresponding to the channel number. λ_f is the disappearance rate of muons bound to nuclei of a given type, and λ_b is the rate of random counts in the electron telescope. In this experiment $\lambda_b \leq 0.005\times10^5$ sec^{-1}, and the multiplicative factor $e^{-n\lambda_b}$ could be approximated by one. The values of the coefficients α_{35} and α_{37} are derived from the isotopic concentrations in the targets and take into account the effects of the finite channel width in the time analyzer and the random phasing between the "start" pulse and the 10-Mc/sec wave train. For the Cl^{35} target, $\alpha_{35} = 0.966$ and $\alpha_{37} = 0.034$; for the Cl^{37} target, $\alpha_{35} = 0.23$ and $\alpha_{37} = 0.77$. λ_f(Ag) has been measured using a pure silver target and found to be (10.92 ± 0.27) per μsec. λ_f(C) has been measured by Reiter et al.[4] and found to be $(4.899 \pm 0.007)\times10^5$ sec^{-1}.

The quantities A, B, C, D, $\lambda_f(35)$, and $\lambda_f(37)$ were calculated using an iterative least-squares program written for the IBM-650 computer. A plot of the data, along with the calculated function, is shown in Fig. 2.

The disappearance rates obtained in this experiment are:

$$\lambda_f(35) = (22.54 \pm 0.52)\times10^5 \text{ sec}^{-1},$$

$$\lambda_f(37) = (17.03 \pm 0.49)\times10^5 \text{ sec}^{-1}.$$

The measurements of Yovanovitch[5] show that in the region of chlorine, the decay rate λ_d is the same as the decay constant of the free muon. Using the value for the decay constant of the positive muon of 4.52×10^5 sec^{-1},[4] we obtain for the capture rates of negative muons in chlorine isotopes:

$$\lambda_c(35) = (18.02 \pm 0.49)\times10^5 \text{ sec}^{-1},$$

$$\lambda_c(37) = (12.51 \pm 0.52)\times10^5 \text{ sec}^{-1}.$$

The ratio $\lambda_c(37)/\lambda_c(35)$ is 0.694 ± 0.034, and the ratio of the difference in the capture rates to the mean value is $[\lambda_c(35) - \lambda_c(37)]/\overline{\lambda} = (36.1 \pm 4.6)\%$.

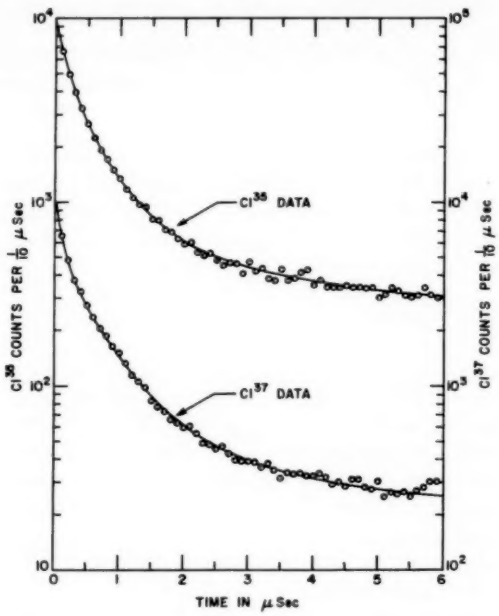

FIG. 2. Decay curves of μ^- mesons in separated chlorine isotopes. The curve is the function obtained by a least-squares fit to the data. Statistical deviations are not shown, but are the square root of the indicated count.

*Work partially supported by the U. S. Atomic Energy Commission.

†Submitted in partial fulfillment of the requirements for the degree of Doctor of Philosophy at the Carnegie Institute of Technology by W. J. Bertram, Jr.

‡National Science Foundation Predoctoral Fellow.

[1]H. Primakoff, Revs. Modern Phys. 31, 802 (1959).

[2]H. A. Tolhoek and J. R. Luyten, Nuclear Phys. 3, 679 (1957).

[3]J. M. Kennedy, Phys. Rev. 87, 953 (1952).

[4]R. A. Reiter et al., Phys. Rev. Letters 5, 22 (1960).

[5]D. D. Yovanovitch, Phys. Rev. 117, 1580 (1960).

FORMATION OF MUONIUM AND OBSERVATION OF ITS LARMOR PRECESSION*

V. W. Hughes, D. W. McColm, and K. Ziock
Gibbs Laboratory, Yale University, New Haven, Connecticut

and

R. Prepost
Nevis Laboratory, Columbia University, New York, New York
(Received June 17, 1960)

After the discovery[1,2] that muons which originate from pion decays are polarized and that positrons which originate from muon decays are emitted with an angular asymmetry with respect to the spin direction of the muons, it was realized[2,3] that it should be possible to observe the atom consisting of a positive muon and an electron (called muonium) and to measure its hyperfine structure. The present Letter reports the formation of muonium in pure argon gas; muonium is observed through its characteristic Larmor precession frequency.

Muonium in its ground $1\ ^2S_{1/2}$ state can be formed when a positive muon is slowed down in matter and captures an electron from an atom in the stopping material. If the muons are polarized, the muonium atoms formed should also have a net polarization.[4] Specifically, if the z axis of quantization is taken along the direction of the momentum of the incident muon beam, then the spin direction of a positive muon will be in the negative z direction to a good approximation.[5] Hence substates $(F, m_F) = (1, -1)$, $(1, 0)$, and $(0, 0)$ will form in the relative amounts 1/2, 1/4, and 1/4, respectively, where F is the quantum number for total atomic angular momentum and m_F is the associated magnetic quantum number. In the states $(1, 0)$ and $(0, 0)$ the muon is unpolarized; the time involved in establishing these unpolarized states subsequent to the electron capture by the muon is determined by the hyperfine structure interaction between the electron and the muon and is of the order of 10^{-10} sec. In the state $(F, m_F) = (1, -1)$ the muon is polarized with its spin along the negative z axis.

Many searches have been made for muonium since 1957. Usually[6,7] the attempt has been to observe the characteristic precession frequency of muonium in the state $(F, m_F) = (1, -1)$ in an external magnetic field H whose direction is perpendicular to the direction of the incoming muon beam (or equivalently to the axis of quantization). The muonium spin angular momentum will precess[8] about H with the frequency $f = \mu H/h$ [μ = magnetic moment of the $(1, -1)$ state of muonium], which is 1.39 Mc/sec-gauss. The published accounts indicate that solid or liquid targets have been used. An experiment has also been done[9] to look for a Zeeman transition between the $F = 1$ magnetic sublevels of muonium induced by a radio-frequency field, when muons are stopped in N_2O gas at 50 atm pressure.

A wide variation has been observed in the amount of depolarization of positive muons stopped in different materials.[6,10,11] The polarization is measured in a precession experiment in which the magnetic field is chosen so as to detect the precession of a free muon; in such an experiment polarized muonium would appear unpolarized because of its high precession frequency. The observed variation in polarization has often been ascribed to varying amounts of muonium formation. However, this explanation is not necessarily correct because one can conceive of other depolarizing mechanisms, e. g., those resulting from chemical reactions of the muon.[12]

The present experiment was designed to search for muonium in pure argon gas at high pressure. The argon gas was contained in a stainless steel cylinder at a pressure of 50 atm and was purified by recirculation over titanium sponge heated to 500°C. First the depolarization of the muons stopped in the gas was measured in a free-muon precession experiment.[1] The value of the ratio of the asymmetry parameter, a, for argon to that for carbon was 0.08 ± 0.15, and thus within the accuracy of the experiment no free polarized muons remain in argon. This result is a necessary condition that all the muons form muonium.

As a specific search for muonium, the characteristic precession frequency of muonium in the state $(F, m_F) = (1, -1)$ was looked for in the manner indicated in Fig. 1. An external magnetic field H between 3 and 5 gauss was applied perpendicular both to the direction of the incoming muon beam and to the direction from the target to the positron telescope, and its value was measured to an accuracy of 1% with an electron reso-

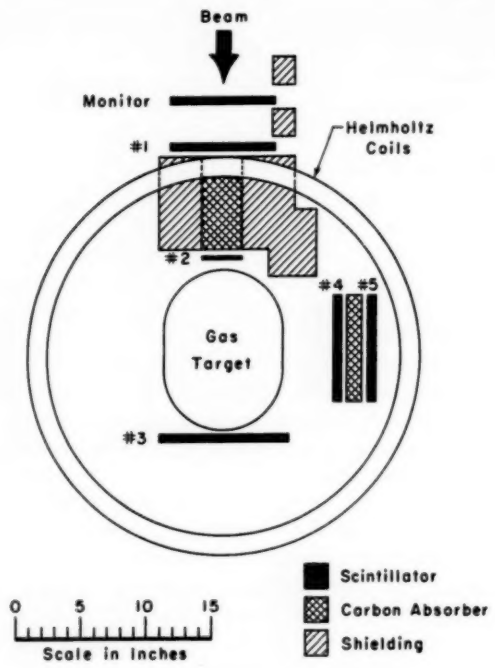

FIG. 1. Experimental arrangement.

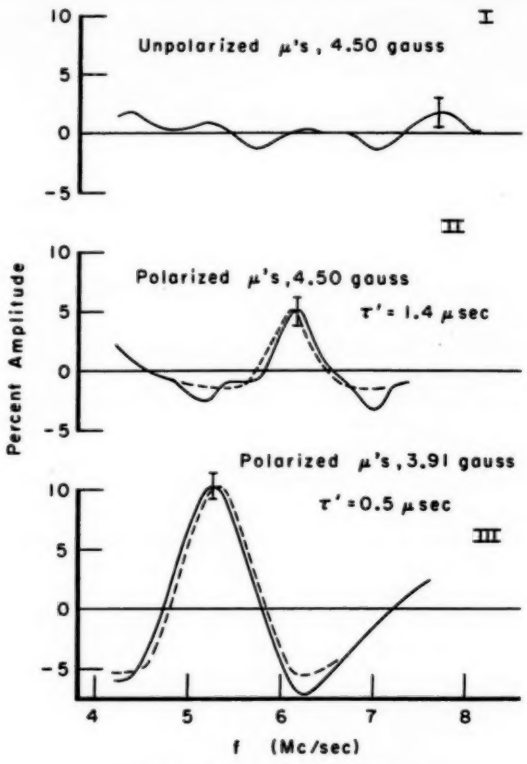

FIG. 2. Frequency analysis.

nance spectrometer using DPH free radicals. The distribution of time intervals between the incoming muon pulses (1-2-$\bar{3}$ coincidences) and those decay positron pulses (4-5 coincidences) which came between 0.2 and 2.0 microseconds after the muon pulse was converted to a spectrum of pulse heights which was fed into a pulse-height analyzer. The characteristic precession of polarized muonium should appear as an oscillation in the pulse-height analyzer data.

The data were assumed to represent the sum of four components, due to (1) polarized muonium, (2) polarized free muons, (3) unpolarized muons, and (4) accidental coincidences. We determined the amplitudes of (2) through (4) by a least squares procedure in which (1), which must be represented by a rapidly varying periodic function, would not contribute. With these computed amplitudes, the contributions of (2) through (4) to the data were then subtracted, leaving numbers y_i containing only the desired oscillation due to polarized muonium. A least squares fit to the y_i was made using the function

$$y_i = e^{-t_i/\tau}\left\{C + Ae^{-t_i/\tau'}\sin[2\pi f(t_i + t_0)]\right\}.$$

Here τ is the muon mean lifetime; τ' is a parameter introduced in order to allow for line broadening, either through field inhomogeneities, drifts in electronics, or depolarization of muonium in collisions; f is the trial value for the precession frequency of the magnetic moment of muonium; t_0 is the time delay between the stopping of the muons and the emission of the earliest positrons used in the data analysis. An IBM-650 computer was used for these computations.

The results of this analysis are shown in Fig. 2 for three sets of data; for two of the cases (II and III) polarized muons were stopped in argon at different magnetic fields and for case I pions were stopped (and hence unpolarized muons were produced). The solid curves were obtained from the analysis of the data and represent the percent amplitude of A compared to the total counting rate. The error bars correspond to an error of one standard deviation in the percent amplitude. The dashed curves are theoretical line shapes centered in each case at the muonium precession frequency predicted from the measured value of the magnetic field. The theoretical lines were

computed with the values of τ' and t_0 determined from the data analysis and were normalized to the peak amplitudes of the lines computed from the data.

Resonances are clearly seen in cases II and III at the frequencies which are predicted for muonium precession on the basis of the magnetic field measurements. The observed and predicted resonance frequencies agree within the experimental uncertainty of 0.2 Mc/sec. The observed amplitudes of the resonances are 4 to 5 standard deviations. In case I where unpolarized muons were used, no resonance is observed. In three other cases, not shown here, where polarized muons were used at different magnetic fields, resonances were observed at the precession frequency of muonium; in one additional case with unpolarized muons, no resonance frequency was found. Hence we concluded that muonium is formed in pure argon. Although it is difficult to relate quantitatively the percent amplitude shown in Fig. 2 to the fraction of muons which form muonium, the data do indicate that close to 100% of the muons form muonium in pure argon.

Muonium is of interest principally because it is the simplest system involving a muon and an electron, and hence it offers the greatest promise for a precise study of the interaction between these two particles and thus for a test of the quantum electrodynamic field theory of the muon, electron, and photon system. In particular, it would be of great value to measure the hyperfine structure separation, $\Delta\nu$, in the ground $1\,^2S_{1/2}$ state of muonium. Under the assumption that the muon is a Dirac particle, the theoretical value for $\Delta\nu$ is given by

$$\Delta\nu = \left\{(\tfrac{16}{3})\alpha^2 c R_\infty \frac{\mu_\mu}{\mu_0}\right\}\left\{1+\frac{m}{M}\right\}^{-3}\left\{1+\frac{\alpha}{\pi}\right\},$$

in which α = fine structure constant, c = velocity of light, R_∞ = Rydberg constant for infinite mass, m = electron mass, M = muon mass, $\mu_0 = e\hbar/2mc$ = Bohr magneton, $\mu_\mu = e\hbar/2Mc$ = muon magneton. The first bracketed term is the Fermi expression; the second term is a reduced-mass correction; the last term includes the lowest order anomalous magnetic moments of the electron and muon. Use of the known values of the atomic constants[13] gives $\Delta\nu = 4464.0$ Mc/sec. The next order α^2 term has not yet been calculated but is, of course, calculable in principle from a Bethe-Salpeter equation for the bound state of the muon and electron.

Comparison of a precise experimental value for $\Delta\nu$ with the theoretical value would provide a critical test of electrodynamics involving the muon and could reveal an anomalous structure of the muon. In view of the abundant formation of muonium that we have found, we are hopeful that a measurement of the hyperfine structure of muonium will be possible and we are preparing to do this experiment.

It is a pleasure to acknowledge encouragement and support from and helpful discussions with Professor L. Lederman and Dr. S. Penman.

---

*This research has been supported in part by the Air Force Office of Scientific Research (with Yale), and also by the Office of Naval Research and the U. S. Atomic Energy Commission (with Columbia).

[1]R. L. Garwin, L. M. Lederman, and M. Weinrich, Phys. Rev. 105, 1415 (1957).

[2]J. I. Friedman and V. L. Telegdi, Phys. Rev. 105, 1681 (1957).

[3]V. W. Hughes, Bull. Am. Phys. Soc. 2, 205 (1957).

[4]G. Breit and V. W. Hughes, Phys. Rev. 106, 1293 (1957).

[5]No direct measurement of the muon spin direction has been made, but measurements of the helicity of the decay positron together with theoretical arguments suggest that the helicity of the positive muon from π decay is negative. If the muon spin were in the $+z$ direction rather than in the $-z$ direction, the labeling of the muonium states would be changed, but none of our conclusions about muonium would be altered. See G. Culligan, S. G. F. Frank, J. R. Holt, J. G. Kluyver, and T. Massam, Nature, 180, 751 (1957); and P. C. Macq, K. M. Crowe, and R. P. Haddock, Phys. Rev. 112, 2061 (1958).

[6]R. A. Swanson, Phys. Rev. 112, 580 (1958).

[7]J. M. Cassels, T. W. O'Keefe, M. Rigby, A. M. Wetherell, and J. R. Wormald, Proc. Phys. Soc. (London) A70, 543 (1957); and J. M. Cassels, Proceedings of the Seventh Annual Rochester Conference on High-Energy Nuclear Physics, 1957 (Interscience Publishers, New York, 1957), Chap. VII, p. 38.

[8]V. Bargmann, L. Michel, and V. L. Telegdi, Phys. Rev. Letters 2, 435 (1959).

[9]D. McColm, V. W. Hughes, A. Lurio, and R. Prepost, Bull. Am. Phys. Soc. 4, 82 (1959).

[10]V. W. Hughes, A. Lurio, D. Malone, L. Lederman, and M. Weinrich, Bull. Am. Phys. Soc. 3, 51 (1958).

[11]M. Weinrich, Ph. D. thesis, Columbia University, 1958 (unpublished).

[12]V. W. Hughes, Phys. Rev. 108, 1106 (1957).

[13]C. M. Sommerfield, Phys. Rev. 107, 328 (1957), and Ann. Phys. 5, 26 (1958). J. W. M. DuMond, Ann. Phys. 7, 365 (1959); R. L. Garwin, D. P. Hutchinson, S. Penman, and G. Shapiro, Phys. Rev. 118, 271 (1960).

OBSERVATION OF π-π RESONANCE IN PION PRODUCTION*

S. D. Drell and F. Zachariasen
Department of Physics, Institute of Theoretical Physics, Stanford University, Stanford, California
(Received June 17, 1960)

The difficulty of obtaining direct experimental information on pion-pion scattering is well known. Goebel and Chew and Low[1] have suggested a procedure to be applied to the process $\pi+N\to\pi+\pi+N$ which involves extrapolating the experimental data into the nonphysical region, to a point at which the pion-pion cross section may be extracted with no theoretical uncertainties. If the experiments can be performed with sufficient accuracy, this is certainly the method of choice for learning about the π-π process, and in particular for seeing whether or not the suggested resonance[2] in the $J=1$, $T=1$ state of the π-π system exists. We would here like to suggest another procedure for finding out if this resonance exists; one which unfortunately is much more beset with theoretical uncertainties and ambiguities than the method of reference 1, but which is perhaps more feasible experimentally.

Our suggestion is based on the analysis of the reactions

$$\gamma+N\to\pi+\pi+N, \tag{1}$$

and

$$\pi+N\to\pi+\pi+N. \tag{2}$$

Let p and p' denote the four-momenta of the initial and final nucleons, respectively; q_1 and q_2, the four-momenta of the two final pions; and k, the four-momentum of the initial photon [process (1)] or pion [process (2)]. What we have in mind is attempting to identify a resonance in the final-state interaction of the two outgoing pions. In general, separating the final-state interaction of the pions from the total process is extremely difficult due to the strong interaction of each pion with the recoil nucleon. However, if the π-N interaction could be held constant, the variations in the cross sections for (1) and (2) would presumably be due to variations in the π-π interaction. It is of course impossible to keep the π-N interaction precisely constant, but by a suitable choice of the kinematics we may hope to reduce the variations produced by it to a minimum.

Let $S=(q_1+q_2)^2$; $S_1=(q_1+p')^2$; and $S_2=(q_2+p')^2$. Then $S(S_1,S_2)$ is the total center-of-mass energy squared of the π-$\pi(\pi_1-N,\pi_2-N)$ system. If we program experiments to hold S_1 and S_2 constant, and vary S, then at least the total center-of-mass energy of each π-N system is held constant. This does not imply that the π-N interaction is held constant for two reasons. First, as the center-of-mass energy of the two pions is changed, the amplitude that the two pions be in a given relative JT state changes due to the π-π interaction, and this alters the amplitude to find either pion in a given state relative to the nucleon. Secondly, there may still be additional changes in the π-N interactions since we are holding only S_1 and S_2 fixed, and these do not uniquely determine the π-N interaction. However, if we choose S_1 and S_2 to be in an energy region—say beyond the first resonance—where the various π-N phase shifts are more or less comparable, there should be no drastic variations due to this. Hopefully, then, as S is varied through the region of the π-π resonance, there will be a peak in the cross sections for (1) and (2) if and only if the π-π resonance exists.[3]

The specific kinematics corresponding to fixing S_1 and S_2 and varying S is most conveniently taken to be the following: In the center-of-mass system of the complete reaction, choose the symmetrical point where $|\vec{q}_1|=|\vec{q}_2|$, and the angles θ_1 and θ_2 are equal, as shown in Fig. 1. Then we have

$$\begin{aligned} S&=2\mu^2+2\omega_1\omega_2-2q_1q_2\cos\theta_{12}\\ &=4\omega^2-4q^2\cos^2\theta=4E\omega+M^2-E^2, \end{aligned} \tag{3}$$

where $|\vec{q}_1|=|\vec{q}_2|=q$, $\theta_1=\theta_2=\theta$, and $\omega^2=q^2+\mu^2$; and where E is the total center-of-mass energy.

Also,

$$\begin{aligned} S_1=S_2&=M^2+\mu^2+2E_{p'}\omega+2p'q\cos\theta\\ &=M^2+\mu^2+2E\omega-4\omega^2+4q^2\cos^2\theta\\ &=M^2+\mu^2+2E\omega-S. \end{aligned} \tag{4}$$

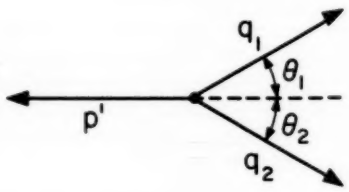

FIG. 1. Angles and momenta for emerging nucleon and pions.

It is clear then, that it is possible to fix S_1 and S_2, and to vary S, provided the total energy E is varied as well.

The energies necessary to cover the interesting region in S, which is roughly[2] $4\mu^2 \leq S \leq 16\mu^2$, are easily obtained from (3) and (4). We may first express S in terms of S_1 and E by inserting (4) in (3): $S = E^2 + M^2 + 2\mu^2 - 2S_1$. Then if we set $S_1 = (M + 3\mu)^2$, corresponding to a π-N center-of-mass energy in the valley beyond the first π-N resonance, we have $S = E^2 - 12M\mu - M^2 - 16\mu^2$. Thus to make S range from $4\mu^2$ to $16\mu^2$, we must make E^2 range from $M^2 + 12M\mu + 20\mu^2$ to $M^2 + 12M\mu + 32\mu^2$. The maximum value of E which is needed is something less than $M + 6\mu$, or about 1175-Mev incident gamma energy in the lab system for process (1), or 1165-Mev incident pion energy in the lab system for process (2).

The size of the peak which should appear in the cross sections for processes (1) and (2) if the π-π resonance does exist is not an easy thing to predict accurately on the basis of present theoretical knowledge and techniques. One thing which will certainly affect the size significantly is the amplitude with which the relative $T = 1$, $J = 1$ state is present in the outgoing two-pion system. It is even conceivable that the bump would be entirely insignificant even if the resonance were present.

It is possible to make a crude estimate of the effect of a π-π resonance on the photoproduction process (1), in order to reassure oneself that there is a reasonable amplitude for the two pions to be in the appropriate state. This estimate is made by grafting part of the effect of the resonance onto the $\gamma + N \to \pi + \pi + N$ amplitude as calculated in the static model,[4] and corresponds to adding to the photoproduction without π-π scattering, Fig. 2(a), an effect such as shown in Fig. 2(b). Formally, this may be done by extracting from the static theory result[4] that part of the amplitude describing the pions in a relative $T = 1$, $J = 1$ state, and multiplying it by $F_\pi(S)$, where F_π is the pion electromagnetic form factor. To see the basis for doing this, let M be the pion production amplitude. Then we may expand $M = \sum_{JT} M_{JT} P_J Q_T$, where P_J and Q_T are projection operators, into the indicated two-pion states. Now write $M_{JT} = (M_{JT} D_{JT})/D_{JT}$, where D_{JT} is the determinantal function[5] for π-π scattering in the TJ state. Considered as a function of S, M_{JT} has singularities from $4\mu^2$ to ∞ but $M_{JT} D_{JT}$ has singularities only from $16\mu^2$ to ∞.[6] Thus it is plausible to expand $(M_{JT} D_{JT})$ in

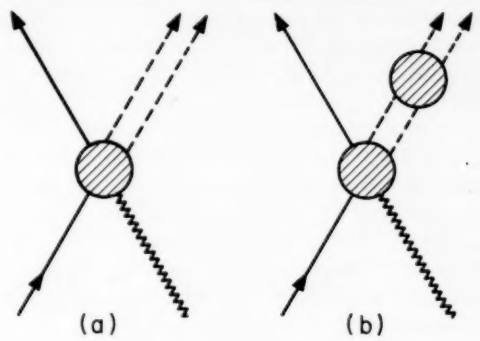

FIG. 2. (a) Diagram for production of two pions (dashed line) by incident gamma ray (wavy line) on nucleon (solid line) without π-π scattering. (b) Modification to include π-π scattering.

powers of the π-π interaction. If we keep just the lowest term in this expansion (corresponding to no π-π interaction) we have $M_{JT} = M_{JT}^{(0)}/D_{JT}$, where $M^{(0)}$ is the production amplitude without π-π scattering. Now, unless $J = 1$ and $T = 1$, there is presumably no π-π resonance, so we may replace D_{JT} by 1 in these cases. However, if $J = 1$ and $T = 1$, $1/D_{11} = F_\pi$,[6] so we have $M_{11} = M_{11}^{(0)} F_\pi$, and therefore $M = M^{(0)} + M_{11}^{(0)}(F_\pi - 1)$.

If $M^{(0)}$ is chosen as the expression resulting from the static theory [Eqs. (15) and (16) of reference 4] and the $J = 1$ state is picked out, taking into account the difference between the pion-nucleon center-of-mass system and the center-of-mass system of the two pions only in the projection operator, then the resulting expression for the $\gamma + p - \pi^+ + \pi^- + p$ cross section is the same as Eq. (17) of reference 4 with the replacements

$$(\tfrac{1}{2}\sin^2\theta_+ + \tfrac{1}{3}) - (\tfrac{1}{2}\sin^2\theta_+ + \tfrac{1}{3})(\tfrac{4}{5}|F_\pi|^2 + \tfrac{4}{5}\mathrm{Re}F_\pi + \tfrac{1}{5}),$$

$$\tfrac{1}{5}(\tfrac{1}{2}\sin^2\theta_- + \tfrac{1}{3}) - (\tfrac{1}{2}\sin^2\theta_- + \tfrac{1}{3})(\tfrac{4}{5}|F_\pi|^2 - \tfrac{4}{5}\mathrm{Re}F_\pi + \tfrac{1}{5}),$$

$$\tfrac{1}{3}(\tfrac{5}{3}\cos\varphi - \cos\theta_+ \cos\theta_-) -$$

$$(\tfrac{5}{3}\cos\varphi - \cos\theta_+ \cos\theta_-)(\tfrac{4}{5}|F_\pi|^2 - \tfrac{1}{5}). \quad (5)$$

Thus in this approximation the two pions are in the resonant state a large fraction of the time. At the Frazer-Fulco value for the π-π resonance $S = 10$ and $|F_\pi|^2 \approx 17$, $\mathrm{Re}F_\pi = 0$. With these parameters we find from (5) that the cross section should be enhanced by a factor of ≈ 14. The half-width of the bump is roughly $5\mu^2$.

This result is not to be interpreted as a reliable

calculation of the pair production cross section including the effects of a π-π resonance. First of all, it is based on the static model which is certainly not accurate at the energies of interest to us here. Secondly, even if the static model were itself sensible, the π-π resonance has been included in only the most primitive way. The only virtue of (5) is that it shows that there are no unexpected factors which tend to damp out the effect of the π-π resonance, and, in this most modest prediction, there is no reason that (5) should be wildly wrong.

It is difficult to make a similar rough estimate for the second reaction, $\pi+N\to\pi+\pi+N$, due to the absence of any plausible starting point such as existed for the photoproduction through the static-theory calculation, which is known to be accurate for low energies.[4] Nevertheless, there is no reason to believe that the effect of the resonance would be completely suppressed in that process either.

There are two remaining comments which can help to isolate the effect of the resonance. The first is that while we cannot calculate much about processes (1) and (2), we can calculate the density of states factor, and the variations produced by it, at least, can be removed from the cross sections. The differential cross section for either process (1) or process (2) will have the form

$$d\sigma=\left(\frac{1}{2\pi}\right)^5\frac{1}{v_{\mathrm{rel}}}\frac{1}{64k_0E_p}\sum_{\substack{\text{spins,}\\ \text{polarizations}}}|M|^2\frac{q^2}{E-2\omega+2\omega\cos^2\theta}\,d\omega_1d\Omega_1d\Omega_2$$

at the symmetrical point defined earlier. Here k_0 and E_p are the initial energies, v_{rel} is the incident relative velocity, M is the invariant Feynman matrix element, and the remaining factors speak for themselves. In terms of the useful variables S, and $S_1(=S_2)$, the density of states factor becomes

$$\frac{q^2}{E-2\omega+2\omega\cos^2\theta}=\frac{(S+S_1-M^2-\mu^2)^2-4\mu^2E^2}{4E^2}\left[\frac{E^2+M^2+\mu^2-S-S_1}{E}+\frac{S+S_1-M^2-\mu^2}{E}\times\frac{(S+S_1-M^2-\mu^2)^2-E^2S}{(S+S_1-M^2-\mu^2)^2-4\mu^2E^2}\right]^{-1}$$

The second comment is that in order to assist in the elimination of variations in the cross section due to processes other than the $J=1$, $T=1$ π-π resonance, it would be useful in process (2) to measure the ratio of cross sections, for example,[1]

$$\sigma(\pi^-+p\to\pi^++\pi^-+n)/\sigma(\pi^++p\to\pi^++\pi^++n),$$

since in the lower process the two final pions always have $T=2$ and are therefore never in the resonant state. In the photoproduction process this taking of ratios cannot be done since there is no way of making the final pions in a pure $T=2$ or $T=0$ state.

The observations of this Letter were triggered by questions of Owen Chamberlain.

*Supported in part by the U. S. Air Force through the Air Force Office of Scientific Research.

[1]G. Chew and F. Low, Phys. Rev. 113, 1640 (1959); C. Goebel, Phys. Rev. Letters 1, 337 (1958).

[2]W. Frazer and J. Fulco, Phys. Rev. 117, 1603 (1960).

[3]Similarly a peak at a π-N resonance should be observed by fixing S and S_2, say, and varying S_1 through a resonance energy for the π-N system. A recent discussion of the π-π resonance in π interactions is given by P. Carruthers and H. A. Bethe, Phys. Rev. Letters 4, 536 (1960).

[4]R. Cutkosky and F. Zachariasen, Phys. Rev. 103, 1108 (1956).

[5]M. Baker, Ann. Phys. 4, 271 (1958).

[6]M. Baker and F. Zachariasen, Phys. Rev. 119, 438 (1960); J. D. Bjorken, Phys. Rev. Letters 4, 473 (1960).

CASCADE TIME OF π^- IN LIQUID HYDROGEN*

T. H. Fields, G. B. Yodh, M. Derrick, and J. G. Fetkovich
Carnegie Institute of Technology, Pittsburgh, Pennsylvania
(Received June 22, 1960)

We report herein a measurement of the time taken by negative pions to go from a velocity of $0.01c$ to nuclear capture in liquid hydrogen. The measurement was undertaken in order to provide direct experimental data on the cascade process, which must be understood for the interpretation of experiments concerning π^- and K^- absorptions at rest in liquid hydrogen.

The experimental method[1] utilized the kinematics of $\pi^- \to \mu^-$ decay in flight to permit measurement of the pion velocity at the instant of decay. As Fig. 1 shows, by measuring the muon laboratory angle and the muon range, one can measure pion velocities down to $\beta\ (=v/c) = 0.01$ (corresponding to $T = 7$ kev), for muon laboratory angles in the backward hemisphere. By so determining the number of π^- which decay with $\beta < 0.01$, and using the known π^- lifetime, the time taken by the pion to go from this velocity to nuclear absorption was determined.

The experimental procedure consisted of scanning hydrogen bubble chamber pictures of a stopping negative pion beam for $\pi^- \to \mu^- \to e^-$ decays. 80 000 negative pions came to rest in the central volume of a 15-cm bubble chamber in a magnetic field of 9 kilogauss. The pictures were scanned twice, and all $\pi^- \to \mu^- \to e^-$ (i.e., two-kinked) tracks for which the film angle between the directions of the first two tracks exceeded 80° were measured and calculated. Every event for which the space angle between the first two tracks exceeded 90° is shown on Fig. 1 as a dot. The scanning efficiency for events with the muon range exceeding 0.5 cm was found to be >90%, and was ~50% for muon ranges of about 0.1 cm. Typical measuring errors are shown on two points. Also, the muon range straggling, as observed in this chamber for $\pi^+ \to \mu^+$ decays at rest, is shown.

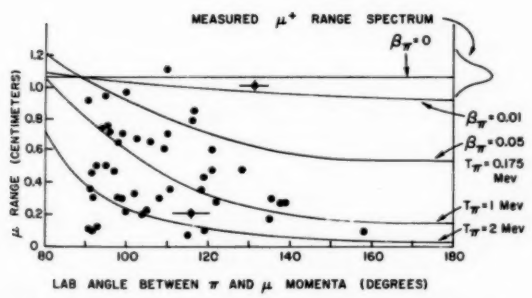

FIG. 1. Kinematics of $\pi \to \mu$ decay in flight. Each dot represents one $\pi \to \mu$ decay found in pictures containing 80 000 π^- stops in liquid hydrogen.

We estimate from Fig. 1 that two $\pi^- \to \mu^-$ decays were observed in the backward hemisphere for which $\beta < 0.01$. This leads to the following expression for the mean time taken by a negative pion in going from $\beta = 0.01$ to nuclear capture:

$$\tau = \left(\frac{2}{80\,000}\right)(2.5\times 10^{-8}\ \text{sec})(2) = (1.2^{+1.2}_{-0.5})\times 10^{-12}\ \text{sec}.$$

The quoted statistical error was determined by calculating the relative probability for obtaining two events for various values of the true time τ. Similarly, one concludes from the graph that the time elapsed between $\beta = 0.05$ and $\beta = 0.01$ is about 2×10^{-12} sec.

As a check on the method, a calculation was made, using ordinary stopping power theory, of the number of events expected in the region 1 Mev $> T >$ 0.175 Mev, laboratory angle exceeding 90°. The result, 27 events, is to be compared with the observed number of 19. The agreement is probably satisfactory, considering the decrease of scanning efficiency for short muon tracks.

Among the sources of systematic error which have been considered and found to be unimportant are: (1) Coulomb scattering of the pion in its last mm of range, (2) absorption of the negative muon by impurities in the chamber, and (3) false events in which the pion underwent nuclear scattering.

The cascade time observed in this experiment is about two orders of magnitude smaller than that which would be required for radiative deexcitation of the $\pi^- p$ atom to the $n = 1$ state.[2] Day, Snow, and Sucher[3] have recently shown that such an effect could arise from Stark effect mixing of various l levels during a collision of the $\pi^- p$ atom with a hydrogen atom, which can lead to rapid nuclear absorption of the pion from s states with $n \approx 4$. In particular, Day[4] has made calculations which yield the following picture for the sequence of events taking place[2]: The pion slows from $\beta = 0.05$ to $\beta = 0.01$ by inelastic collisions with atomic electrons in $\approx 2.8\times 10^{-12}$ sec. Then the

pion, through further inelastic collisions, is captured from the continuum in about 0.9×10^{-12} sec. A π^-p atom with $n\approx30$ is formed, and de-excites to $n\approx15$ by collisions in which H_2 molecules are dissociated, in $\approx0.2\times10^{-12}$ sec. At $n\approx15$, the predominant mode of energy loss becomes Auger transitions in collisions, which can de-excite the π^-p atom to $n\approx4$ in $\approx1.0\times10^{-12}$ sec. At this point the Stark effect mixing and consequent nuclear capture from s states happens[5] in $<\approx10^{-12}$ sec, a much shorter time than would be required for further de-excitation via Auger collisions or via radiation.

The present data are in reasonable agreement with the above picture[6] of pion absorption from s states via Stark effect mixing. They therefore imply the absence of mesonic x rays from low-lying levels of the π^-p atom.

We wish to thank John Deahl and Gale Pewitt for help in running the chamber, and Anna Marie Bankowski for scanning the pictures.

*This work was supported in part by the U. S. Atomic Energy Commission.

[1]T. Fields, G. B. Yodh, M. Derrick, and J. Fetkovich, Bull. Am. Phys. Soc. 4, 401 (1959).

[2]A. S. Wightman, Phys. Rev. 77, 521 (1950); and Princeton University thesis, 1949 (unpublished).

[3]T. B. Day, G. A. Snow, and J. Sucher, Phys. Rev. Letters 3, 61 (1959).

[4]T. B. Day, invited paper at 1960 American Physical Society Washington Meeting, and University of Maryland Physics Department Report No. 175 (unpublished).

[5]J. E. Russell and G. L. Shaw, Phys. Rev. Letters 4, 369 (1960).

[6]A crucial part of the above picture is the rapid de-excitation of the π^-p atom to $n\approx4$. Wightman's (reference 2) original upper limit for the de-excitation time was 5×10^{-11} sec. An investigation of the implications of this value in view of the present experimental result was reported by T. B. Day, G. A. Snow, and J. Sucher, Phys. Rev. 118, 864 (1960). However, the rapid de-excitation (1.2×10^{-12} sec) calculated in reference 4 seems to allow fairly good agreement with this experiment without invoking other absorption mechanisms.

EFFECTIVE-RANGE FORMULA FOR PHOTOPION PRODUCTION FROM PIONS*

How-Sen Wong
Lawrence Radiation Laboratory, University of California, Berkeley, California
(Received June 27, 1960)

In the Chew-Mandelstam[1] approach to the strong-interaction problem at low energies, the amplitude for $\gamma+\pi\to2\pi$ plays a central role in any phenomena involving photons. Recently, Ball[2] has found that this process produces an additive correction to the formulas of Chew et al.[3] for photopion production from nucleons. Compton scattering by pions and by nucleons also involves the $\gamma+\pi\to2\pi$ reaction. A simple and reasonably accurate formula for the $\gamma+\pi\to2\pi$ amplitude which can be used in any of these applications is given here.

We assume that the simple invariant transition amplitude, $M(s,t,u)$, has the Mandelstam representation[4]

$$M(s,t,u)=\frac{1}{\pi^2}\int_4^\infty\int_4^\infty\rho(x,y)\left[\frac{1}{(x-s)(y-t)}+\frac{1}{(x-t)(y-u)}+\frac{1}{(x-u)(y-s)}\right]dx\,dy. \quad (1)$$

It is defined through the relation,

$$T_{fi}=\frac{i(2\pi)^4\delta^4(K+p_1-p_2-p_3)\sum[(-i/\sqrt{2})\epsilon_{\alpha\beta\gamma}\epsilon_{\lambda\sigma\mu\nu}(p_1)_\lambda(p_2)_\sigma K_\mu\epsilon_\nu]M(s,t,u)}{(16p_{10}p_{20}p_{30}K)^{1/2}}, \quad (2)$$

where α, β, and γ are the isotopic indices of the pions, and $\epsilon_{\alpha\beta\gamma}$ and $\epsilon_{\lambda\sigma\mu\nu}$ are the conventional antisymmetric tensors of third and fourth rank, respectively. Here s, t, and u are defined[5] as (see Fig. 1)

$$s=-(K+p_1)^2,$$
$$t=-(K-p_2)^2,$$
$$u=-(K-p_3)^2, \quad (3)$$

and are related by the condition

$$s+t+u=3.$$

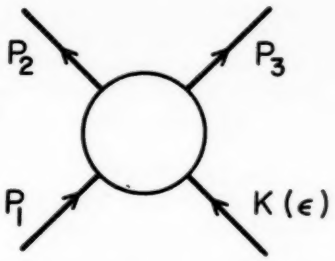

FIG. 1. Diagram of $\gamma+\pi\rightarrow 2\pi$.

When the photon K and meson p_1 are the incoming particles, the variables s, t, and u are related to barycentric system variables,

$$s=4(1+p^2),$$

$$t=1-2kE+2kp\cos\theta,$$

$$u=1-2kE-2kp\cos\theta,$$

where p and E are the magnitudes of the outgoing pion momenta and energy, respectively, k is the energy of the photon, and we have $\cos\theta=(\vec{p}\cdot\vec{k})/pk$. The formula for the differential cross section in the barycentric system is

$$\frac{d\sigma}{d\Omega}=\sum\frac{p}{k}\left|\frac{1}{8E}\,\frac{T_{fi}}{2\pi}\right|^2.$$

From the Mandelstam representation, we can locate the singularities of the partial-wave amplitudes, defined through the relation

$$M(s,z)=\sum_{\text{odd}\,l}M_l(s)P_l'(z),$$

where $z=\cos\theta$. The M_l's are analytic in the whole complex s plane except for cuts on the real axis. The right-hand cut runs from 4, the physical threshold for two pions, to ∞; the left cut runs from 0 to $-\infty$. Using these analytic properties, the unitary condition, and the Omnés[6]-Frazer-Fulco[7] method, we find

$$M_l(s)=\frac{1}{\pi D_l(s)}\int_{-\infty}^{0}\frac{D_l(s')\,\mathrm{Im}M_l(s')}{s'-s}\,ds', \qquad (4)$$

where $D_l(s)$ is the π-π denominator function introduced by Chew and Mandelstam.[1]

If we assume that for $s\geq 4$, we have $\mathrm{Im}M\approx\mathrm{Im}M_1$, we can show that

$$M(s,t,u)\approx\frac{1}{\pi}\int_4^\infty\mathrm{Im}M_1(x)\left[\frac{1}{x-s}+\frac{1}{x-t}+\frac{1}{x-u}\right]dx. \qquad (5)$$

We see that all partial waves for $l>1$ can be obtained once M_1 is known. Formula (5) is the basis of an independent calculation that has been carried out by Gourdin and Martin.[8]

Using crossing symmetry, we can obtain a formula for $\mathrm{Im}M_1(s)$ for $s<0$ in terms of $\mathrm{Im}M_1(s)$ for $s>4$. We do not give this formula here because the effect-range approach does not require such detailed information. In any event, it is clear that for $l=1$, the integral of Eq. (4) is homogeneous, so that its solution is not unique, at least with respect to a multiplicative factor. Therefore an arbitrary parameter must be introduced. In the calculation below, we shall fix this parameter Λ as the value of $M_1(s)$ at $s=1$. At present, we do not know how to relate Λ to fundamental constants, and for the time being it must be determined from experiment.

To proceed further, we need the denominator function, D_1, for p-wave pion-pion scattering. The pion-pion calculations of Chew and Mandelstam have not yet reached a conclusive stage but these authors have given an approximate form for D_1 which corresponds to the replacement of the unphysical branch cut in the pion-pion amplitude by a finite number of poles.[9] Further, they have shown that two poles lead to an accurate approximation in the physical region up to $s\sim 40$. Once the parameters of the two-pole formula have been determined, it will be a straightforward problem to incorporate the information into the amplitude $\gamma+\pi\rightarrow 2\pi$. The determination of the pion-pion parameters is still in progress,[10] but we outline here, for future use, the form of solution of our problem that corresponds to the pole approximation of Chew and Mandelstam.[9] We shall illustrate the method with the one-pole pion-pion amplitude, for which parameters have been given by Frazer and Fulco.[7]

We propose to replace the left-hand cut of the amplitude M_1 by poles with appropriate positions and residues. The "n-pole formula" thus obtained contains $2n$ parameters. One of these may be identified with Λ; the rest will be determined from crossing relations.

By representing $\mathrm{Im}M_1$ on the left-hand cut by one or two delta functions, we obtain from Eq. (4) the one-pole formula

$$M_1(s)=\frac{\Lambda(1+a)D_1(1)}{(s+a)D_1(s)}, \qquad (6)$$

or the two-pole formula

$$M_1(s)=\frac{\Lambda D_1(1)}{D_1(s)}\left[\frac{D_1(-b)}{s+b}+\frac{\Lambda_1 D_1(-c)}{s+c}\right]\times\left[\frac{D_1(-b)}{1+b}+\frac{\Lambda_1 D_1(-c)}{1+c}\right]^{-1}, \qquad (7)$$

where Λ and Λ_1 are real, and a, b, and c are real and positive. The parameters Λ_1, a, b, and c may be determined from the following crossing relations which are derived from Eq. (5):

$$M_1(1) - \tfrac{3}{2} M_1^{\,L}(1) = 0, \tag{8a}$$

$$\frac{\partial}{\partial s} M_1(1) = 0, \tag{8b}$$

$$\frac{\partial^2}{\partial s^2} M_1(1) - 6 \frac{\partial^2}{\partial s^2} M_1^{\,L}(1) = 0, \tag{8c}$$

where

$$M_1^{\,L}(s) = \frac{1}{\pi} \int_{-\infty}^{0} \frac{\operatorname{Im} M_1(s')ds'}{s' - s}$$

$$= \frac{\Lambda(1+a)D_1(1)}{(s+a)D_1(-a)}$$

for the one-pole formula, and

$$M_1^{\,L}(s) = \Lambda D_1(1)\left[\frac{1}{s+b} + \frac{\Lambda_1}{s+c}\right]\left[\frac{D_1(-b)}{1+b} + \frac{\Lambda_1 D_1(-c)}{1+c}\right]^{-1}$$

for the two-pole formula.

If the Frazer-Fulco one-pole $D_1(s)$ function is used for a resonance at $s = 10$, we find $a \cong 5.7$ from the crossing condition (8a). The parameters Λ_1, b, and c in the two-pole formula may be determined from (8a) to (8c). It turns out that no choice of Λ_1, b, and c can satisfy all three conditions (8a) to (8c) if the Frazer-Fulco one-pole formula is used. However, the first two conditions of Eqs. (8) can be satisfied with the pair of poles in the range between 0 and -4.93. The p-wave amplitude in the physical region not only is insensitive to the positions of the two poles so long as (8a) and (8b) are satisfied, but also is not much different from the one-pole solutions, which satisfies (8a) alone. Thus we may be confident of the accuracy of the two-pole results once the parameters of the two-pole π-π scattering formula are known. The one-pole formula already obtained is probably adequate for most purposes.

We can estimate the order of magnitude of Λ by considering the decay of neutral pions, assuming that the $\gamma + \pi \rightarrow 2\pi$ reaction plays a prominent role in the intermediate state. We find $|\Lambda| \approx 1.3e$ ($e^2 = 1/137$) if the π^0 lifetime is 4×10^{-16} sec.[11] Our calculation is based on the assumption that only the least massive (two-pion) intermediate state contributes to the dispersion integral, but there is no good reason to neglect the 3π contribution, especially if there is a resonance or a bound state at roughly the same energy as the two-pion resonance.[12] A better estimate of Λ may come from photopion production on nucleons, where Ball has shown that $\gamma + \pi \rightarrow 2\pi$ makes an important and characteristic contribution.[2]

The author wishes to thank Professor G. F. Chew for suggesting this investigation and for his guidance. He also wishes to thank Dr. D. Y. Wong and Dr. A. Martin for helpful discussions.

* A preliminary account of this work was given at the 1959 Thanksgiving meeting of the American Physical Society, November 27-28, 1959 [Bull. Am. Phys. Soc. 4, 407 (1959)]. This work was performed under the auspices of the U. S. Atomic Energy Commission.

[1]G. F. Chew and S. Mandelstam, Phys. Rev. 119, 467 (1960).

[2]J. S. Ball, University of California Radiation Laboratory Report UCRL-9172 (unpublished); and J. S. Ball, following Letter [Phys. Rev. Letters 5, 73 (1960)].

[3]G. F. Chew, M. L. Goldberger, F. E. Low, and Y. Nambu, Phys. Rev. 106, 1337 (1957).

[4]S. Mandelstam, Phys. Rev. 112, 1344 (1958); 115, 1741 and 1752 (1959).

[5]We use the fundamental metric tensor such that $p_1 \cdot p_2 = \vec{p}_1 \cdot \vec{p}_2 - p_{10} p_{20}$. Units are used in which $\hbar = c = 1$ and $\mu = 1$, where μ is the mass of the pion.

[6]R. Omnès, Nuovo cimento 8, 316 (1958).

[7]W. R. Frazer and J. R. Fulco, Phys. Rev. Letters 2, 365 (1959); Phys. Rev. 117, 1909 (1960).

[8]M. Gourdin and A. Martin, CERN Report No. 7687 TH/67 (unpublished).

[9]G. F. Chew and S. Mandelstam, University of California Radiation Laboratory Report UCRL-9126 (unpublished).

[10]J. S. Ball and D. Y. Wong, Lawrence Radiation Laboratory (private communication).

[11]G. Harris, J. Orear, and S. Taylor, Phys. Rev. 106, 327 (1957).

[12]G. F. Chew, Phys. Rev. Letters 4, 142 (1960). The author wishes to thank Professor R. J. Eden of Cambridge University for indicating this point to him.

EFFECT OF THE PION-PION RESONANCE ON THE NEGATIVE-POSITIVE RATIO

James S. Ball
Lawrence Radiation Laboratory, University of California, Berkeley, California
(Received June 27, 1960)

It has been shown by Frazer and Fulco that a P-wave pion-pion resonance can account for the isotopic vector component of the nucleon electromagnetic structure.[1] The purpose of this note is to show that the contribution of this resonance to photoproduction is capable of producing a large effect in the π^- to π^+ ratio at threshold.

It is assumed that the Chew, Goldberger, Low, and Nambu invariant amplitudes,[2] $A^{\pm 0}$, $B^{\pm 0}$, $C^{\pm 0}$, and $D^{\pm 0}$, satisfy the Mandelstam representation.[3] The singularity produced by the 2π state is a branch cut running from $4\mu^2$ to ∞ in the complex plane for the momentum-transfer variable $t=-(q-k)^2=(\omega_q-k)^2-(\vec{q}-\vec{k})^2$.[4] Since G parity allows only the scalar part of the photon interaction in the process $\gamma+\pi\to\pi+\pi$, the 2π singularities will be present only in the photoproduction amplitudes representing the scalar part of the photon, namely the (0) amplitudes. It should also be noted that the (0) amplitudes have only the $I=1/2$ pion-nucleon phases in the physical region for $\gamma+n\to n+\pi$ and $\gamma+\bar{n}\to\bar{n}+\pi$. The strength of the singularities associated with these two channels is given by the imaginary part of the amplitudes. Therefore, since the $I=1/2$ phases are small in the low-energy region for photoproduction, it is a good approximation to neglect these singularities.

The (0) amplitudes may now be written in the form

$$A^{(0)}(s,t)=\text{Poles}+\frac{1}{\pi}\int_{4\mu^2}^{\infty}dt'\,\frac{\mathrm{Im}_2A^{(0)}(s,t')}{t'-t}, \quad (1)$$

where Im_2 denotes the absorptive part of $A^{(0)}$ for the channel $\gamma+\pi\to n+\bar{n}$. The square of the total energy for this channel is t, and s is the square of the total energy for the photoproduction channel. Since the singularities are neglected for $s>(M+\mu)^2$, the physical region for photoproduction, a polynomial expansion may be used to continue $\mathrm{Im}_2A^0(s,t')$ to $s>(M+\mu)^2$.

By means of the unitarity condition, it is now possible to obtain $\mathrm{Im}_2A^0(s,t)$ expressed in terms of the helicity amplitudes for $\pi+\pi\to n+\bar{n}$, and $\pi+\gamma\to\pi+\pi$. Since the process $\pi+\gamma\to\pi+\pi$ contains only odd angular momentum, only the $J=1$ state is kept, and $J\geq 3$ is neglected. The $\pi+\pi\to n+\bar{n}$ states that enter into these imaginary parts are the same as those in the nucleon electromagnetic structure problem, and we find

$$\mathrm{Im}A^0=-th(t)g_2^{\,v}(t), \quad (2a)$$

$$\mathrm{Im}B^0=h(t)g_2^{\,v}(t), \quad (2b)$$

$$\mathrm{Im}C^0=0, \quad (2c)$$

and

$$\mathrm{Im}D^0=h(t)g_1^{\,v}(t), \quad (2d)$$

where

$$h(t)=\frac{3}{8\sqrt{2}e}\,\frac{m_1^{\,*}(t)}{F_\pi(t)},$$

$m_1(t)$ is the $J=1$ eigenamplitude for $\pi+\gamma\to\pi+\pi$ and $g_1^{\,v}$, $g_2^{\,v}$ are the imaginary parts of the nucleon form factors given by FF. Here $F_\pi(t)$ is the pion form factor introduced by these authors.

Wong has shown that $m_1(t)$ is well represented for $t>4\mu^2$ by the form

$$m_1(t)=\frac{\Lambda}{F_\pi(1)}\left(\frac{1+a}{t+a}\right)F_\pi(t), \quad (3)$$

where Λ is the new coupling constant required to describe $\pi+\gamma\to\pi+\pi$ and a is a parameter that depends on the pion-pion P-wave amplitude. If the FF pion-pion resonance is used, we have $a=5.7$ and $F_\pi(1)=1.08$.

Because of the simple form of $h(t)$, it is possible by making suitable subtractions in FF's Eq. (1) to write the dispersion-integral parts of A^0, B^0, C^0, and D^0 directly in terms of the nucleon isotopic vector form factors. Since the form factors are approximately linear in the region $-5<t<0$, the (0) amplitudes may be expressed in terms of $G_i^{\,v}(0)$ and

$$\frac{1}{G_i^{\,v}(0)}\,\frac{dG_i^{\,v}(t)}{dt}\bigg|_{t=0}=\frac{1}{\frac{1}{6}\bar{r}^2}=\frac{1}{t_\gamma'},$$

where t_γ' is approximately the position of the pion-pion resonance. (Frazer and Fulco ob-

tained $t_\gamma' \approx 12$.)[1] For the (0) amplitudes, we have

$$A^0 = \frac{e_\gamma g_\gamma}{2}\left[\frac{1}{s-M^2}+\frac{1}{\bar{s}-M^2}\right] + \lambda'\left(\frac{\mu_p'-\mu_n}{2}\right)\left[1+\frac{t-a}{t_\gamma'}\right], \quad (4a)$$

$$B^0 = \frac{e_\gamma g_\gamma}{(s-M^2)(\bar{s}-M^2)} - \lambda'\left(\frac{\mu_p'-\mu_n}{2}\right)\frac{1}{t_\gamma'}, \quad (4b)$$

$$C^0 = -\tfrac{1}{2}g_\gamma(\mu_{p_\gamma}'+\mu_{n_\gamma})\left[\frac{1}{s-M^2}-\frac{1}{\bar{s}-M^2}\right], \quad (4c)$$

$$D^0 = -\tfrac{1}{2}g_\gamma(\mu_{p_\gamma}'+\mu_{n_\gamma})\left[\frac{1}{s-M^2}+\frac{1}{\bar{s}-M^2}\right] - \lambda'\frac{e}{2t_\gamma'}, \quad (4d)$$

where $\bar{s} = -(p_2 - k)^2$ and

$$\lambda' = \frac{3\Lambda(1+a)}{8\sqrt{2}\,eF_\pi(1)}.$$

Since the (0) amplitudes enter into $d\sigma(\pi^+)$ and $d\sigma(\pi^-)$ with opposite signs, the ratio $d\sigma(\pi^+)/d\sigma(\pi^-)$ at threshold will be quite sensitive to changes in the (0) amplitude. The threshold ratio becomes

$$R = \frac{d\sigma(\pi^-)}{d\sigma(\pi^+)} = \left(\frac{ef+(\mu_p+\mu_n)f-\frac{\lambda'}{8\pi}(\mu_p'-\mu_n)\left(1-\frac{1+a}{t_\gamma'}\right)}{ef-(\mu_p+\mu_n)f+\frac{\lambda'}{8\pi}(\mu_p'-\mu_n)\left(1-\frac{1+a}{t_\gamma'}\right)}\right)^2 \quad (5)$$

An upper limit on the magnitude of Λ can be obtained by considering π^+ production separately. It is observed that a change in f^2 of ± 0.01 (which is roughly the current uncertainty) can be compensated for in the threshold π^+ cross section by giving Λ a value of $\mp 1.75e$. The experimental errors in the present π^+ data, with $f^2 = 0.08$, would seem to allow $-1.8e < \Lambda < 1.8e$ (see Fig. 1). When combined with the uncertainty in f^2, this would constrain $|\Lambda|$ to be less than $2.5e$.

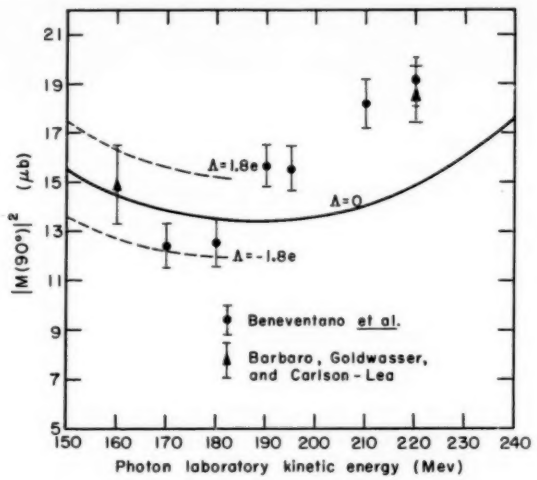

FIG. 1. The matrix element squared for π^+ photoproduction at $\theta = 90$ deg. The solid line represents the prediction for $\Lambda = 0$; the dashed lines, for $\Lambda = \pm 1.8e$. The experimental points are those of Barbaro et al. and Beneventano et al. (see reference 6).

Wong[5] has estimated the size of Λ from the π^0 lifetime. His results are $|\Lambda| \approx e$. For $|\Lambda| = e$, formula (5) leads either to $R = 1.16$ or to $R = 1.44$, depending on the sign of Λ.

The author is greatly indebted to Professor Geoffrey F. Chew for suggesting this investigation and for his constant advice throughout the course of this work. The author would also like to thank Dr. How-sen Wong for making some of his results available prior to publication.

[1]W. R. Frazer and J. R. Fulco, Phys. Rev. 117, 1609 (1960) (hereafter denoted FF).

[2]G. F. Chew, M. L. Goldberger, F. E. Low, and Y. Nambu, Phys. Rev. 106, 1345 (1957) (hereafter denoted CGLN).

[3]S. Mandelstam, Phys. Rev. 112, 1344 (1958); 115, 1741 and 1752 (1959).

[4]The notation of CGLN is used throughout.

[5]H. S. Wong, Bull. Am. Phys. Soc. 4, 407 (1959); and preceding Letter [Phys. Rev. Letters 5, (1960)].

[6]A. Barbaro, E. L. Goldwasser, and D. Carlson-Lee, Bull. Am. Phys. Soc. 4, 273 (1959); M. Beneventano, G. Bernardini, D. Carlson-Lee, G. Stoppini, and L. Tau, Nuovo cimento 4, 323 (1956).

ERRATUM

PLASMA STABILITY AND BOUNDARY CONDITION. F. C. Hoh [Phys. Rev. Letters 4, 559 (1960)].

Reference 9 should be replaced by: [9]B. B. Kadomtsev and A. V. Nedospasov, J. Nuclear Energy (to be published).

The third last paragraph, beginning "The above discussions are valid for ..." should be replaced by the following paragraph:

"In contradiction to the present theory, Kadomtsev and Nedospasov[9] have proposed that diffusion waves develop inside a positive column when the magnetic field and the electron current along it exceed certain critical values. Their theory fits the experiments[7,11] well, but is certainly in disagreement with Bostick and Levine's observations.[5] A similar theory, i.e., ion wave instability theory, for a fully ionized plasma has also been proposed[4] to explain the instability in the *B*-3 Stellarator.[8]"

ABSTRACTS

In this section are printed the abstracts of Articles that have been forwarded to The American Institute of Physics for publication in THE PHYSICAL REVIEW. In quoting information obtained from this section before the appearance of the corresponding Article, reference should be made to "Physical Review (to be published)" rather than to this Journal.

DAMPING OF A TORSIONALLY OSCILLATING CYLINDER IN LIQUID HELIUM AT VARIOUS TEMPERATURES AND DENSITIES.

Benjamin Welber, Lewis Research Center, National Aeronautics and Space Administration, Cleveland, Ohio (Received September 25, 1959; revised manuscript received April 21, 1960).

A method is described for measuring the product of the viscosity and the density of liquid helium by determining the energy dissipation of a piezoelectric cylinder of quartz oscillating in a torsional mode. Data are reported for liquid helium under its own vapor pressure as well as at higher densities.

INDUCED AND SPONTANEOUS EMISSION IN A COHERENT FIELD. III.

I. R. Senitzky, U. S. Army Signal Research and Development Laboratory, Fort Monmouth, New Jersey (Received November 9, 1959).

The theory developed in the first two articles of this series, dealing with the interaction between the electromagnetic field in a cavity resonator and a number of two-level molecules, is generalized to include a Gaussian spread in the molecular frequency. The center of the molecular frequency distribution coincides with the cavity resonant frequency. There is a coherent driving field in the cavity at the same frequency, and cavity loss is taken into account.

Using the formalism previously developed for a quantum-mechanical field in a lossy cavity, expressions are obtained by means of second-order perturbation theory for the expectation values of the field strength and field energy in the cavity, and of the power loss by the molecules. It is shown that the parts of the field energy resulting from induced and spontaneous emission, respectively, initially increase as the square of the time and approach steady-state values after (different, in general) transient periods, each of which is determined by two time constants: cavity relaxation time and inverse molecular frequency spread.

It is also shown that both the induced and spontaneous emission power radiated by the molecules increase initially linearly with the time and approach steady-state values after transient periods. For the induced emission power, the transient period is determined by only one time constant, the inverse molecular frequency spread, while for the spontaneous emission power it is determined both by the inverse molecular frequency spread and the cavity relaxation time. The ratio of induced to spontaneous emission is initially n, and approaches a steady-state value $n[\exp(r^2)(1 - \operatorname{erf} r)]^{-1}$, where n is the driving field energy in units of the photon energy, and r is the ratio of the cavity resonance width to molecular frequency spread. The seeming inconsistency of this value with the classical value of the ratio of the Einstein coefficients is discussed.

STATISTICAL MECHANICS OF LIQUID He^4.

Ryoichi Kikuchi,* Harry H. Denman, and Charles L. Schreiber,† Department of Physics, Wayne State University, Detroit, Michigan (Received May 4, 1960).

The partition function proposed by Feynman for liquid He^4, based on his path integral method, is evaluated for a simple cubic lattice considering long-range permutations as well as nearest-neighbor permutations (to which the previous analysis by one of the authors was restricted). The result indicates a second-order phase transition at the λ point. The marked improvements over the previous treatment are: (1) the specific heat behaves as T^3 near absolute zero, (2) the specific heat peak is more pronounced at the λ point, and (3) when triangles are added as possible finite polygons above T_λ the specific heat just above T_λ increases over the previous result, showing an improvement. Equating the theoretical λ point with the experimental one, a value for the effective mass of a helium atom about 1.6 times the normal mass is obtained.

*Now at Hughes Aircraft Company, Malibu, California.

†Now at Department of Physics, University of California, Los Angeles, California.

IRREVERSIBILITY IN INTERACTING SPIN SYSTEMS. J. Philippot,* Institute for Fluid Dynamics and Applied Mathematics, University of Maryland, College Park, Maryland (Received May 11, 1960).

A system whose Hamiltonian is split into two terms $\mathcal{H}=\mathcal{H}_0+\lambda V$ exhibits two types of irreversible processes. The first processes are described by $\mathcal{H}_0$ alone; only the second processes, which result from the perturbation, lead to an increase of the entropy of the system. These processes are illustrated by the examples of free precession and cross relaxation. General formulas are given for transition probabilities and the expressions applied to cross relaxation in LiF agree with the results obtained by Bloembergen and Pershan.

*On leave of absence from the University of Brussels, Brussels, Belgium.

SPIN RELAXATION OF F-CENTER ELECTRONS. W. E. Blumberg,* Department of Physics, University of California, Berkeley, California (Received January 27, 1960).

Several possible mechanisms leading to spin transitions in the electron-nuclear spin system of an F-center electron and its neighboring nuclei have been examined. Calculations show that the most probable transition is one in which the electron spin changes but the nuclear spin does not change, and which results from the second-order perturbation of the spin-orbit coupling of the electron due to lattice vibrations. The spin-lattice relaxation time of the F-center electrons in NaCl at 300°K has been measured at 70, 2950, and 8300 gauss. The relaxation time is 2×10^{-6} second, independent of the magnetic field, in approximate agreement with the theory.

*Present address: Bell Telephone Laboratories, Murray Hill, New Jersey.

MEASUREMENT OF F-CENTER CONCENTRATION AND RELAXATION TIME BY MICROWAVE FARADAY ROTATION. Dale Teaney, W. E. Blumberg,* and A. M. Portis, Department of Physics, University of California, Berkeley, California (Received January 27, 1960).

The use of a bimodal cavity for the observation of electron spin resonance is described. The two samples of NaCl containing F centers used by Blumberg are investigated by electron spin resonance. Their F-center concentrations are found to be 4.4×10^{17} and 2.3×10^{18} electrons/cm^3, respectively. The spin-lattice relaxation time at room temperature of the F-center electrons is found to be 1.7 microseconds.

*Present address: Bell Telephone Laboratories, Murray Hill, New Jersey.

LORENZ NUMBER FOR HIGH-PURITY COPPER. G. K. White and R. J. Tainsh, Division of Physics, Commonwealth Scientific and Industrial Research Organization, Sydney, Australia (Received May 13, 1960).

Following a recent report that the Lorenz number, $L=\lambda/\sigma T$, does not approximate to the theoretical value of $2.45\times10^{-8}W$ ohm deg^{-2} for very pure copper at the lowest temperatures, measurements have been made of thermal and electrical conductivities on copper of similar purity. Between 2 and 4°K, values of L are observed lying in the range 2.5_4 to $2.4_0\times10^{-8}W$ ohm deg^{-2}.

RELATION BETWEEN X-RAY COLORATION AND OPTICAL BLEACHING OF KCl CRYSTALS. W. E. Bron, International Business Machines Research Center, Yorktown Heights, New York (Received May 6, 1960).

Changes in the absorption of KCl crystals in the spectral region of 200 mμ to 1000 mμ have been observed during room temperature x-ray irradiation and subsequent bleaching with F light. It is observed that both coloration and bleaching of the F band occurs in two stages. Secondary centers such as M, R, and V_3 centers grow primarily during the second stage of coloration, and the rate of growth of these centers during the second stage is enhanced by plastic deformation in a manner similar to that of the F band. It is found that the absorption change at the F band during the first stage of bleaching approximately equals that during the first stage of coloration. Furthermore, the initial rate of bleaching of the F band is proportional to the initial F-band absorption in samples irradiated only into the first stage of coloration, but is essentially independent of the initial F-band absorption in samples irradiated into the second stage of coloration. It is concluded from this and other evidence that the center responsible

for the first stages of coloration and bleaching differs from the center responsible for the second stages of coloration and bleaching. A major point of difference is that the first-stage centers are considered to be located in the bulk of the crystal, whereas the second-stage centers are located in the vicinity of dislocations.

It is also observed that M centers which are formed from F centers during the first stage of bleaching can be bleached with F light. To explain the observations concerning this M-band bleaching, it is proposed that M as well as F centers are bleached when they are joined by mobile defects, possibly vacancy pairs. Some of the second-stage centers located in the vicinity of dislocations are thought to compete with the centers located in the bulk of the crystal for the mobile defects.

DEPENDENCE OF THE OPTICAL BLEACHING RATE OF X-IRRADIATED KCl CRYSTALS ON LIGHT INTENSITY. W. E. Bron and W. R. Heller, International Business Machines Research Center, Yorktown Heights, New York (Received May 6, 1960).

Measurements have been made on the changes in the bleaching rate of the F band as the result of varying the intensity of F light. Bleaching was done on KCl crystals which had been irradiated at room temperature with hard x-rays into either the first or second stage of coloration. In the first-stage irradiated crystals, the total bleaching of the F centers during the first ten seconds of illumination varied approximately linearly with light intensity at low intensities, but became saturated at intensities greater than 5×10^{14} photons/sec cm^2. The bleaching process is thought to occur primarily through the capture of photoelectrons at pre-existing electron traps. Based on this model it is possible to set up the kinetic equations for the bleaching process. Using reasonable values for photoelectron capture coefficients forces one to conclude that the number of photoelectrons is always very small throughout the bleaching process. The resulting simplification in the analysis of the kinetic equations leads to a prediction of the experimentally observed variation of the initial bleaching rate with light intensity. The analysis shows that the ratio of the capture coefficient for photoelectrons of the electron trapping centers to that of negative-ion vacancies is about unity, which strongly suggests that the trapping centers are either traps with net positive charge or are neutral traps located close to the original F centers.

The rate of bleaching during the second stage of bleaching saturated at the lowest intensity used which was about 1×10^{14} photons/sec cm^2. This result is discussed in terms of the analysis given for the first stage of bleaching.

POSSIBILITY OF THE EXISTENCE OF ATTRACTIVE FORCES BETWEEN DISLOCATIONS OF LIKE SIGN. J. Weertman, Department of Metallurgy and Materials Science, Technological Institute, Northwestern University, Evanston, Illinois (Received April 8, 1960).

It is concluded that two moving dislocations of the same sign and on the same slip plane can sometimes attract rather than repel one another (and two of unlike sign repel rather than attract each other). This reversal over the usual behavior will occur at velocities where the kinetic energy in the displacement field of an isolated moving dislocation is larger than the strain energy in the same field.

BEHAVIOR OF THE PRINCIPAL ELASTIC MODULI AND SPECIFIC HEAT AT CONSTANT VOLUME OF KCl AT ELEVATED TEMPERATURES. Frank D. Enck, University of Maryland, College Park, Maryland, and Franklin and Marshall College, Lancaster, Pennsylvania (Received January 25, 1960; revised manuscript received April 25, 1960).

Measurements of the adiabatic elastic constants of potassium chloride (KCl) have been made in the region 300°K to the melting point (1043°K) by a dynamical method developed by Balamuth. Recently determined values of the specific heat at constant pressure (C_p) have been used to calculate the isothermal values of the compressibility. Values of the specific heat at constant volume (C_v) have been obtained, using recent values of the coefficient of thermal linear expansion (α), the above-mentioned values of C_p, and the isothermal compressibilities. The results indicate that there is a slight rise in C_v above the Dulong-Petit value above 725°K. This rise is not significant, since the estimated error interval incloses the Dulong-Petit value, and

consequently the Dulong-Petit law is most likely valid up to the melting point.

MAGNETOACOUSTIC OSCILLATIONS AND THE FERMI SURFACE IN ALUMINUM. B. W. Roberts, General Electric Research Laboratory, Schenectady, New York (Received April 11, 1960).

Measurements of magnetoacoustic attenuation in very pure aluminum have been made with 10 to 100 Mc/sec longitudinal sound waves in magnetic fields up to 9200 oe at a temperature of 4.2°K. The observed oscillations, or geometric resonances, for various crystal and field orientations may be interpreted utilizing the second zone of the nearly free electron Fermi surface model proposed by Harrison. The data suggest regions of high scattering near [100] portions of the surface that prevent the observation of periods for some orbit configurations.

DIELECTRIC CONSTANT OF A DENSE ELECTRON GAS. T. Pradhan and P. Misra, Department of Physics, Ravenshaw College, Utkal University, Cuttack, India (Received November 17, 1959).

The problem of absorption and dispersion of electromagnetic waves in a dense electron gas is treated semiclassically through the use of the Boltzmann equation and Fermi-Dirac statistics. The singularity in the dispersion formula is treated by the method of Van Kampen. Expressions for the dielectric constant and conductivity as functions of frequency have been obtained for temperatures at and near absolute zero.

CHANGE IN STRUCTURE OF BLUE AND GREEN FLUORESCENCE IN CADMIUM SULFIDE AT LOW TEMPERATURES. L. S. Pedrotti, Air Force Institute of Technology, Wright-Patterson Air Force Base, Ohio, and D. C. Reynolds, Aeronautical Research Laboratories, Wright-Patterson Air Force Base, Ohio (Received May 11, 1960).

The two fundamental fluorescences observed in cadmium sulfide crystals subjected to ultraviolet excitation at low temperatures are classified according to wavelength. Photographs of the two fluorescences at 4.2°K and 77°K are given, and their structures are compared. Experimental evidence on the change in structure of the green emission near 5130 A between 4.2°K and 77°K is presented and used to confirm an explanation for the apparent "green" shift in cadmium sulfide proposed by Thomas and Hopfield.

ANISOTROPIC CONDUCTION IN NONSTOICHIOMETRIC RUTILE (TiO_2). Lewis E. Hollander, Jr., and Patricia L. Castro, Lockheed Aircraft Corporation, Palo Alto, California (Received May 2, 1960).

Measurements are reported for the anisotropic conductivity in rutile for different nonstoichiometric compositions. This anisotropy, ρ_a/ρ_c, has a peak in excess of 10 000 to 1 and is a maximum at the nonstoichiometric composition corresponding to $\rho_c = 10^3$ ohm cm. Based on these data, it is proposed that for very nonstoichiometric material, impurity band conduction predominates, and as the material is made more stoichiometric, a transition to conventional conduction via the conduction band occurs. This transition occurs at very different nonstoichiometric compositions for the two crystal directions. Thus, a large anisotropy is observed in the intermediate region.

EFFECT OF SHEAR ON IMPURITY CONDUCTION IN n-TYPE GERMANIUM. H. Fritzsche, Department of Physics and Institute for the Study of Metals, University of Chicago, Chicago, Illinois (Received May 6, 1960).

Shear strains, which change the donor wave functions, greatly affect impurity conduction, which depends sensitively on the wave function overlap of neighboring impurity states. The change of impurity conduction of germanium containing 5.2×10^{15} antimony atoms per cc and about 3% compensation was measured at 1.9°K as a function of shear strains produced by uniaxial tension and compression along [110]. It is shown that the anisotropy and the saturation of the conductivity changes observed at stresses larger than 4×10^8 dynes/cm^2 can be understood from the strain-induced changes of the donor-state wave functions.

METALLIC TRANSITIONS IN IONIC CRYSTALS: SOME GROUP-THEORETICAL RESULTS. M. Flower, N. H. March, and A. M. Murray, Department of Physics, The University, Sheffield, England (Received April 3, 1960).

In view of a discrepancy between results available in the literature, the problem of finding the different irreducible representations for points on the surface of the Brillouin zone in NaCl and CsCl type lattices is re-examined for particular points of high symmetry. The lattice harmonics to be included in cellular-type calculations are listed up to and including $l=10$ for two points on the surface of the Brillouin zone in each case. Our results confirm the earlier work of Bell up to $l=6$, and extend her tables somewhat. The present findings however are at variance with Behringer's work on LiH for one of the points (W) which he considers.

PRESSURE SHIFTS IN THE HYPERFINE STRUCTURE CONSTANT OF POTASSIUM. Arnold L. Bloom, Varian Associates, Palo Alto, California, and John B. Carr, U. S. Naval Postgraduate School, Monterey, California (Received May 13, 1960).

Optical pumping and detection methods were used to determine the resonant frequency of the K^{39} $m=0 \rightarrow m=0$ hyperfine line in various environments. Frequency shifts were observed in noble gases and in hydrogen; no shift was observed from a paraffin wall coating. The shifts, expressed as fractional changes in the hyperfine frequency, are similar to those in rubidium though generally somewhat smaller. The hyperfine constant itself was determined for both K^{39} and K^{41}.

COLLISIONS OF ELECTRONS WITH HYDROGEN ATOMS. V. EXCITATION OF METASTABLE 2S HYDROGEN ATOMS. R. F. Stebbings, Wade L. Fite, David G. Hummer,* and R. T. Brackmann, John Jay Hopkins Laboratory for Pure and Applied Science, General Atomic, San Diego, California (Received May 9, 1960).

Ground-state hydrogen atoms produced by thermal dissociation in a tungsten furnace were excited by collision with electrons having energies up to 600 ev. Those atoms which were excited to the metastable $2S$ state were subsequently quenched in an electrostatic field, and the resulting Lyman-alpha radiation was detected with an iodine-vapor-filled photon counter. In order to assign absolute cross-section values to the excitation function obtained in this way, the ratio of the $2S$ to the $2P$ excitation cross sections was determined. From previously obtained knowledge of the cross section for excitation to the $2P$ state, the absolute $2S$ cross section was evaluated. Agreement with the Born approximation was observed at high energies. The angular distribution of the scattered $2S$ atoms was also investigated for electron energies up to 600 ev.

*Present address: Department of Physics, University College, London, England.

IRON SERIES HARTREE-FOCK CALCULATIONS. II. R. E. Watson,* Solid-State and Molecular Theory Group, Massachusetts Institute of Technology, Cambridge, Massachusetts (Received May 9, 1960).

Analytic Hartree-Fock calculations have been carried out for the lowest neutral atom $3d^{n-2}4s^2$ states of Ti through Zn. Except for Cr and Cu, these calculations are for the neutral atom ground states. The results are compared with the earlier $3d^n$ state calculations. It is observed that the $4s$ electrons have little effect on the $3d$ and inner shells.

*Now at AVCO, Research and Advanced Development Division, Wilmington, Massachusetts.

EVIDENCE FOR 0^+ AND 1^- LEVELS IN U^{234} POPULATED IN THE ONE-MINUTE BETA DECAY OF Pa^{234}. G. T. Wood,* Institute for Theoretical Physics, University of Copenhagen, Copenhagen, Denmark (Received May 2, 1960).

A directional correlation measurement has been performed on the 250-kev vs (751 + 795)-kev composite cascade in U^{234} following the 24-day beta decay of Th^{234} and the subsequent one-minute beta decay of Pa^{234}. The "770"-kev (751 + 795 kev) composite photopeak spectrum coincident with the 250-kev gamma ray was displayed on a multichannel pulse-height analyzer for different positions of the scintillation counters. From these spectra the directional correlations between the 250-kev gamma ray and the lower and

upper sides of the 770-kev composite line were measured. The results together with other measurements are consistent with assignments of multipolarity $E1$ to the 250-, 751-, and 795-kev gamma rays and spin and parity assignments $0^+ - 1^- - 2^+$ and $0^+ - 1^- - 0^+$ to the levels involved in the 250-751 kev and 250-795 kev gamma-gamma cascades, respectively. Thus, new levels are proposed at 795 and 1046 kev with spin and parity 1^- and 0^+, respectively.

*Present address: University of Pennsylvania, Philadelphia, Pennsylvania.

NUCLEAR STRUCTURE EFFECTS IN Cs^{133}. M. K. Ramaswamy, Department of Physics, The Ohio State University, Columbus, Ohio (Received April 20, 1960).

The 79-kev transition in Cs^{133}, which is known to be l forbidden ($\Delta l = 2$) magnetic dipole ($M1$), has been analyzed for penetration effects suggested by Church and Weneser. A value of 6.5 ± 2.6 is found for λ, the ratio of the matrix element due to the penetration of the atomic electron into the nucleus and the matrix element due to $M1$ gamma emission. This value of λ is to be compared with the range 5-10 obtained by Church and Weneser for l-forbidden ($\Delta l = 2$) transitions using empirical gamma matrix elements and single-particle wave functions to evaluate the electron matrix element.

ELASTIC SCATTERING OF FAST NEUTRONS BY TRITIUM AND He^3. J. D. Seagrave, L. Cranberg, and J. E. Simmons, Los Alamos Scientific Laboratory, University of California, Los Alamos, New Mexico (Received May 9, 1960).

Differential cross sections have been obtained for the elastic scattering of neutrons by tritium and by He^3 at $E_n = 1.0$, 2.0, 3.5, and 6.0 Mev over the angular range 27° to 161° in the c.m. system. The Los Alamos large Van de Graaff accelerator and pulsed-beam time-of-flight facility were employed, and the scattering samples were contained in small thin-walled stainless steel spheres. One-third mole of He^3 was contained at 5000 psi and one-half mole of tritium was prepared in the form of CaT_2. Absolute cross sections were determined from a comparison with the scattering from a thin shell of CH_2 at each energy, together with calibration of the relative sensitivity of the detector as a function of energy by the known forward yield of the $T(p,n)He^3$ reaction. The angular distributions for n-T scattering are in excellent agreement with the calculations of Bransden, Robertson, and Swan based on a Serber exchange force. The n-He^3 measurements favor qualitatively the Serber rather than the symmetrical exchange force used in the calculations, but the agreement is poorer than that obtained for n-T scattering. The polarization of elastically scattered 1-Mev neutrons was found to be less than 5% for both samples, unlike the strong polarization observed in n-He^4 scattering.

STUDIES OF DECAY SCHEMES IN THE OSMIUM-IRIDIUM REGION. II. DECAY OF 12-DAY Ir^{190}. W. R. Kane* and G. T. Emery,* Lyman Laboratory of Physics, Harvard University, Cambridge, Massachusetts, and Brookhaven National Laboratory, Upton, New York, and G. Scharff-Goldhaber and M. McKeown, Brookhaven National Laboratory, Upton, New York (Received May 13, 1960).

Spectra of the gamma rays and internal conversion electrons emitted in the decay of 12-day Ir^{190} have been studied in detail. Internal conversion spectra were obtained with the aid of double-focusing and intermediate-image beta spectrometers, and a permanent-magnet spectrograph. Gamma-ray spectra were obtained by means of photoelectric conversion, employing a double-focusing spectrometer, and by scintillation techniques.

These measurements of the energies and relative intensities of gamma rays and internal conversion electrons give internal conversion coefficients for a number of transitions. These data, coupled with coincidence studies of gamma rays, support the level scheme reported by Nielsen et al. for Os^{190} and establish new, odd-parity levels at 1384, 1568, and 1876 kev. An upper limit of 2×10^{-5} is set on positron branching in the decay of Ir^{190}. Relative electron capture transition probabilities for the decay of Ir^{190} to Os^{190} and ratios of reduced transition probabilities for electromagnetic transitions from a number of levels of Os^{190} follow from these results. They are compared with the predictions of the strong-coupling model and the asymmetric rotor model. The half-life of Ir^{190}

was found to be 12.3 ± 0.4 days. Even-A iridium-osmium total disintegration energies are found to rise substantially above the values predicted by semiempirical mass formulas, suggesting a possible effect of the change in the nuclear deformation in this region.

*Now at Brookhaven National Laboratory, Upton, New York.

RATIO OF ASYMMETRIC TO SYMMETRIC FISSION OF Pu^{239} AND Pu^{241} AS A FUNCTION OF NEUTRON ENERGY. R. B. Regier, W. H. Burgus, R. L. Tromp, and B. H. Sorensen, Atomic Energy Division, Phillips Petroleum Company, Idaho Falls, Idaho (Received May 2, 1960).

Further radiochemical experiments have been carried out to test the theoretical suggestion that in low-energy neutron-induced fission, the asymmetric to symmetric fission ratio should depend on the spin of the fissioning nucleus. In the present work two kinds of experiments were done. In the first, with both Pu^{239} and Pu^{241}, comparisons were made of the asymmetric/symmetric yield ratios for thermal fission with the corresponding ratios for gross resonance fission with epi-Sm neutrons. In the second kind, monoenergetic neutrons were employed to study variations of Pu^{239} fission yields with neutron energy over the 0.297-ev resonance. If the assumption is made that spin difference is the principal cause of change in the asymmetric/symmetric ratio in this energy region, the results indicate that this ratio differs by a factor of at least 5.3 between the two spin states of Pu^{239}. This is the largest effect of this kind observed to date.

ELASTIC SCATTERING OF HEAVY IONS BY GOLD AND BISMUTH. H. L. Reynolds and E. Goldberg, Lawrence Radiation Laboratory, University of California, Livermore, California, and D. D. Kerlee, Seattle Pacific College Institute for Research, Seattle, Washington (Received April 25, 1960).

The angular distributions of C^{12}, N^{14}, O^{16}, and Ne^{20} elastically scattered by Au^{197} and Bi^{209} have been measured at laboratory energies of approximately 10.4 Mev per nucleon. The elastically scattered ions were recorded in photographic emulsions at laboratory angles from 19° to 175°. In general, measurements were extended only to angles where the ratio of the cross section to the Coulomb cross section, σ/σ_C, was greater than 0.1. In one case the measurement was extended to a region where $\sigma/\sigma_C \leq 1.4\times10^{-4}$. The cross sections all exhibited a behavior similar to that previously reported for C^{12} on Au^{197}. An oscillation in the cross-section ratio occurring at smaller angles than the 20% to 30% rise and sudden drop was observed. Excellent agreement was obtained with the Blair "sharp-cutoff" calculations for values of $\sigma/\sigma_C > 0.2$. Nuclear interaction distances calculated by fitting the sharp-cutoff calculations are consistent with $r_0 = 1.46$ fermis, where $R = r_0(A_1^{1/3} + A_2^{1/3})$. No striking distinction can be made regarding the surface characteristics of the four projectiles or the two targets.

PARITY-NONCONSERVING INTERNUCLEON POTENTIALS. II. EFFECTS IN ELECTROMAGNETIC TRANSITIONS. R. J. Blin-Stoyle,* Department of Physics and Laboratory of Nuclear Science, Massachusetts Institute of Technology, Cambridge, Massachusetts (Received May 9, 1960).

A detailed investigation is made of the way in which parity-nonconserving (PNC) internucleon potentials lead to parity impurities in nuclear states and hence to pseudoscalar asymmetries in the emission of gamma radiation. Explicit expressions are obtained for the angular distribution of unpolarized radiation (a) in emission from nuclei polarized by non-nuclear methods, (b) in β-γ angular correlations, (c) in polarized thermal neutron capture radiation and also for the magnitude of the circular polarization of radiation from an arbitrarily oriented nuclear system. The magnitudes of these effects are then estimated for the case of a transition between low-lying nuclear states and also for a ground-state transition following neutron capture. Finally a critique of the γ-ray transitions so far used in experimental investigations of PNC effects is given. It is concluded that many transitions in particularly simple nuclei are insensitive to PNC effects and that at present all that can be stated with any confidence is that $\mathcal{F} \leq 10^{-4} - 10^{-5}$.

*On Sabbatical leave from the Clarendon Laboratory, Oxford, England.

ANGULAR DISTRIBUTIONS OF THE $D(d,n)He^3$ REACTION FOR 5- TO 12-Mev DEUTERONS. Murrey D. Goldberg and James M. Le Blanc, Lawrence Radiation Laboratory, University of California, Livermore, California (Received April 21, 1960).

The absolute differential cross section for production of monoenergetic neutrons by the $D(d,n)He^3$ reaction has been measured with 5.0, 7.6, 9.6, and 12.2-Mev deuterons. A proton recoil counter telescope was used to detect the neutrons and to separate neutrons from the $D(d,np)D$ breakup reaction. The angular distributions at all energies are very peaked in the forward direction, with a first minimum around 30 to 40 degrees and a subsequent smaller maximum. The angular distributions, transformed to the center-of-mass system, have been fitted with the exchange stripping theory of Owen and Madansky, in which stripping from both incident and target deuterons is formally included. Excellent fits were obtained, but it was necessary to decrease monotonically the interaction radius, R_0, with incident deuteron energy. The variation was considerable, from $R_0 = 8.4 \pm 0.2$ fermis at 5.0 Mev to $R_0 = 5.5 \pm 0.2$ fermis at 12.2 Mev. An isotropic contribution of about 3 mb/sr was added to each distribution to obtain the best fit.

HEAVY-ISOTOPE ABUNDANCES IN MIKE THERMONUCLEAR DEVICE. H. Diamond, P. R. Fields, C. S. Stevens, M. H. Studier, S. M. Fried, M. G. Inghram, D. C. Hess, G. L. Pyle,* J. F. Mech, and W. M. Manning, Argonne National Laboratory, Lemont, Illinois and A. Ghiorso, S. G. Thompson, G. H. Higgins, and G. T. Seaborg, Radiation Laboratory and Department of Chemistry, University of California, Berkeley, California and C. I. Browne, H. L. Smith, and R. W. Spence, Los Alamos Scientific Laboratory, Los Alamos, New Mexico (Received May 2, 1960).

The November 1, 1952, thermonuclear explosion ("Mike") produced all of the uranium isotopes U^{239}, U^{240}, ... U^{255} through multiple neutron capture by U^{238}. The long-lived products of successive β^- decays from these isotopes were measured mass-spectrometrically and radiometrically. The logarithms of the abundances decline smoothly with increasing mass number; the even-mass abundances slightly exceed the geometric mean of adjacent odd-mass abundances. Some nuclear properties of neutron-rich heavy nuclides, not subject to ordinary investigation, are inferred.

*Currently at White Sands Proving Ground, White Sands, New Mexico.

LOW-ENERGY FISSION OF RHENIUM AND TANTALUM: POSSIBLE EFFECT OF NUCLEAR DISTORTION ON ASYMMETRIC FISSION. R. D. Griffioen and J. W. Cobble, Department of Chemistry, Purdue University, Lafayette, Indiana (Received February 15, 1960; revised manuscript received March 25, 1960).

Absolute fission cross sections of natural rhenium and tantalum induced by 30-45 Mev helium ions were determined radiochemically. The mass yield curves of both elements are primarily symmetric above 40 Mev. An asymmetric fission mode becomes apparent at lower energies and is more probable than the symmetric mode at 30-Mev excitation in rhenium. The average number of neutrons emitted is very small, being about two in the 41-Mev bombardment of rhenium. The results, suggesting that the shape and deformability of the fissioning nucleus determine the relative probabilities for asymmetric and symmetric fission, are discussed in view of different current theories of asymmetric fission.

ATOMIC-BEAM MEASUREMENT OF THE HYPERFINE STRUCTURE AND NUCLEAR MOMENTS OF IODINE-131. Edgar Lipworth, Hugh L. Garvin,* and Thomas M. Green,† Lawrence Radiation Laboratory and Department of Physics, University of California, Berkeley, California (Received May 11, 1960).

The nuclear magnetic dipole and nuclear electric quadrupole interaction constants a and b have been measured in 8-day iodine-131 by an atomic beam magnetic resonance experiment. The results are $a = 575.903 \pm 0.006$ Mc/sec, $b = 578.866 \pm 0.075$ Mc/sec. The zero-field hyperfine splittings computed from these values of a and b are $\Delta\nu(5,4) = 3292.99 \pm 0.09$ Mc/sec, $\Delta\nu(4,3) = 2138.22 \pm 0.05$ Mc/sec, $\Delta\nu(3,2) = 1314.24 \pm 0.07$ Mc/sec. The nuclear magnetic dipole moment and nuclear electric quadrupole moment are calculated as $\mu_{131} = 2.738 \pm 0.001$ nm, $Q_{131} = (-0.41 \pm 0.01) \times 10^{-24}$ cm^2. The value of μ_{131} ob-

tained here differs slightly from that obtained by other workers, while the value of Q confirms an earlier measurement made by a different method.

*Present address: John Jay Hopkins Laboratory for Pure and Applied Science, General Atomic Division of General Dynamics Corporation, San Diego, California.

†Present address: Boeing Aircraft Company, Seattle, Washington.

REACTION $C^{14}(p,n)N^{14}$. J. K. Bair, R. D. Edge, and H. B. Willard, Oak Ridge National Laboratory, Oak Ridge, Tennessee (Received April 25, 1960).

The reaction $C^{14}(p,n)N^{14}$ has been studied up to 5-Mev bombarding proton energy with good resolution using targets of high isotopic enrichment. Levels previously unseen in this reaction were found at proton energies of 3.19 Mev ($\Gamma = 6$ kev), 3.38 Mev ($\Gamma = 24$ kev), 3.63 Mev ($\Gamma = 13$ kev), 3.89 Mev ($\Gamma = 35$ kev), 4.19 Mev ($\Gamma = 112$ kev), 4.24 Mev ($\Gamma = 27$ kev), 4.61 Mev ($\Gamma = 140$ kev), and 4.93 Mev ($\Gamma = 106$ kev). Excitation curves at three angles in the region of 2.9-Mev proton energy show the effect of the previously known $J = \frac{3}{2}^-$ ($\Gamma = 80$ kev) resonance interfering with a level of opposite parity. Effects of the nearby $J = \frac{7}{2}^-$ ($\Gamma = 40$ kev) level are not seen, presumably due to the low penetrability of the outgoing F-wave neutron. The thresholds for the second and third neutron groups were investigated using a lithium iodide detector. A new threshold, that for production of the third neutron group, was measured to be 4.910 ± 0.008 Mev in agreement with the known energy of the second excited state in N^{14}.

LEVEL STRUCTURE OF N^{14}. J. K. Bair, H. O. Cohn, and H. B. Willard, Oak Ridge National Laboratory, Oak Ridge, Tennessee (Received April 25, 1960).

Yields and angular distributions of the gamma rays from the first and second levels in C^{13} following excitation by inelastic proton scattering have been measured. Levels are observed at bombarding proton energies 3.80 Mev ($\Gamma = 100$ kev), 4.1 Mev ($\Gamma = 150$ kev), 4.14 Mev, and 4.52 Mev ($\Gamma = 150$ kev). The first three levels result in excitation of the first excited state and the last in excitation mainly of the second excited state of C^{13}. N^{14} excitation energies corresponding to these levels are 11.07 Mev, 11.3_5 Mev, 11.39 Mev, and 11.74 Mev. Possible spin and parity assignments are made on the basis of the γ-ray angular distribution of the 4.52-Mev level. The $C^{13}(p,n)N^{13}$ neutron yield has been re-run yielding better values of the resonant energies. Neutron angular distributions are given for several bombarding proton energies.

CLASSICAL ANALYSIS OF THE REACTION $Be^9(Li^7, Li^8)Be^8$. Samuel K. Allison, Enrico Fermi Institute for Nuclear Studies, University of Chicago, Chicago, Illinois (Received May 9, 1960).

The mechanism of the reaction $Be^9(Li^7, Li^8)Be^8$, $Q = 0.36$ Mev, from which the angular distribution of Li^8 has been measured by Norbeck, Blair, Pinsonneault, and Gerbach (NBPG), is analyzed from a classical viewpoint. The reaction is one of neutron pickup by the Li^7, and it is assumed that due to the low reaction energy and relatively low mass of the neutron the Li^7 and Be^9 are not unrecognizably perturbed from the classical hyperbolic orbits they would follow under Coulomb repulsion. For the NBPG data taken at 2-Mev Li^7 bombarding energy, it is noted that the blurring of the classical trajectories due to diffraction is about 37% in the angle of deviation. Comparison of NPGB's cross sections per steradian for Li^8 formation with those calculated from Rutherford's formula shows that 1 in 10^6 passing Li^7 nuclei can capture a neutron from Be^9 in encounters in which the perinuclear distance is as great as $(3.0 \pm 0.55) \times 10^{-12}$ cm.

The rate of radial attenuation of the probability of finding the Be^9 neutron in unit volume is determined from the angular distribution of Li^8, using the classical equation for the perinuclear separation as a function of angular deviation. In the region $(1.5 < r < 3) \times 10^{-12}$ cm it is consistent with the slope of the function $nr^{-2} \exp(-2\beta r)$ with $\beta = (2.1 \pm 0.5) \times 10^{12}$ cm^{-1}. The theoretical value for a neutron bound to a Be^8 structure by $W_n = 1.63$ Mev is $(2\mu W_n)^{1/2}/\hbar$ or 2.6×10^{12} cm^{-1}.

It is shown that the extraordinarily low (n,γ) cross section for Li^7 determined by Imhoff, Vaughn, Johnson, and Walt cannot be used here to describe the capture. Using a plausible cross section of 5×10^{-25} cm^2, the value of n in the specified region is 1.3×10^{13} cm^{-1}, giving, for instance, the absolute value of neutron probabil-

ity per cm³ at 2.0×10^{-12} cm radius as 6.2×10^{32} cm^{-3}.

The function $nr^{-2}\exp(-2\beta r)$ must join on to one less steep at a radius $\geq 8\times10^{-13}$ cm, or the neutron probability integrated over all space becomes greater than unity.

9.0-Mev GAMMA-EMITTING LEVEL IN C^{12}. D. E. Alburger and R. E. Pixley, Brookhaven National Laboratory, Upton, New York (Received May 5, 1960).

An energy level in C^{12} at 9.0 ± 0.1 Mev has been detected by means of (p,γ,γ) coincidence measurements on the $B^{10}(He^3,p)C^{12}$ reaction at $E_{He^3}=2.2$ Mev. This state decays by a gamma-gamma cascade through the 4.43-Mev first excited state. An upper limit of 5% is placed on the ground-state gamma-ray transition. The intensity of the proton group leading to the 9.0-Mev state (followed by gamma-ray emission) is (0.21 ± 0.07)% relative to the proton branch to the 4.43-Mev level. Gamma-ray branches from the 15.10- and 12.78-Mev states in C^{12} to the 4.43-Mev level have been determined as (4 ± 1)% and (20 ± 7)%, respectively, relative to the corresponding ground-state transitions. The radiations from the 9.0-Mev level have prevented a sensitive search from being made for the 3.2-Mev gamma radiation from the 7.66-Mev level in C^{12} by means of this reaction.

PRODUCTION OF STRANGE PARTICLES BY 1.5-Bev π^- MESONS IN C, Fe, and Pb. Theodore Bowen, Judson Hardy, Jr.,* George T. Reynolds, C. R. Sun, Guido Tagliaferri,† and Albert E. Werbrouck, Princeton University, Princeton, New Jersey, and William H. Moore, Brookhaven National Laboratory, Upton, New York (Received March 17, 1960).

The production of Y^0 (Λ^0, Σ^0), θ^0, Σ^- particles by 1.5-Bev π^- mesons has been observed in a multiplate cloud chamber with one-half inch plates of C, Fe, and Pb. The fraction of inelastic nuclear interactions which result in strange particle production remains approximately constant from C to Pb, with the following yields: Y^0, 1.7 ± 0.4%; θ^0, 1.4 ± 0.5%; Σ^-, 0.2 ± 0.1%. The production angular and momentum distributions are given, along with the distributions obtained from Monte Carlo calculations which do not include secondary interactions of the strange particles.

The yields of hyperons and θ^0's are close to those expected on the basis of the known cross sections in elementary $\pi^- p$ collisions. However, the Σ^-/Y^0 ratio is observed to be much less than expected, indicating at least geometric cross section for $\Sigma^- + p \rightarrow Y^0 + n$.

The following lifetimes were obtained: Λ^0, $(2.72^{+0.29}_{-0.27})\times10^{-10}$ sec; θ_1^0, $(1.09^{+0.18}_{-0.15})\times10^{-10}$ sec. No statistically significant Λ^0 decay asymmetries (up-down, forward-backward, decay proton scattering) were found. Four likely and two possible examples of θ_2^0 interactions were observed, in good agreement with the number expected if the interaction cross section were geometric.

*Now at Westinghouse Electric Corporation, Pittsburgh, Pennsylvania.

†Now at the Università di Milano, Milano, Italy.

PRODUCTION OF STRANGE PARTICLES BY 2.8-Bev PROTONS IN C, Fe, AND Pb. Theodore Bowen, Judson Hardy, Jr.,* George T. Reynolds, Guido Tagliaferri,† and Albert E. Werbrouck, Palmer Physical Laboratory, Princeton University, Princeton, New Jersey, and William H. Moore, Brookhaven National Laboratory, Upton, New York (Received March 17, 1960).

Observations of Λ^0, θ_1^0, and $\Sigma_\pi^\pm$ particles from 2.8-Bev proton interactions have been made in a multiplate cloud chamber with one-half inch plates of C, Fe, and Pb. The $Y^0(\Lambda^0,\Sigma^0)$ and θ^0 cross sections, when compared with those observed for production by 1.5-Bev π^- mesons with the identical arrangement, are lower by at least a factor of four for C and a factor of two for Pb. Production of $\Sigma_\pi^\pm$'s by protons and pions seem to be of comparable magnitude in either C or Pb. Since protons are less effective than pions of similar kinetic energy (in the center-of-mass system) in producing strange particles, it is estimated in the case of incident protons that indirect production of strange particles by intermediate pions accounts for (40^{+28}_{-13})% of the observed particles in C and (64^{+21}_{-14})% in Pb. The different A dependence of the proton and pion cross sections for producing observable strange particles (Λ^0, θ_1^0, $\Sigma_\pi^\pm \rightarrow \pi^\pm + n$) may be fitted by a total proton-nucleon direct production cross section of 0.09 ± 0.06 mb.

The proton-produced strange particle events were used to compute what would be expected when decay γ rays emitted at 90° to the beam direction are observed in the geometry used by Berley and Collins. The predicted decay curve is in excellent agreement with their observations, and the absolute and relative yields agree within the estimated experimental uncertainties.

*Now at Westinghouse Electric Corporation, Pittsburgh, Pennsylvania.
†Now at the Università di Milano, Milano, Italy.

ASSOCIATED PRODUCTION IN PROTON-PROTON COLLISIONS. E. Ferrari, Istituto di Fisica dell' Università, Roma, Italia, and Istituto Nazionale di Fisica Nucleare, Sezione di Roma, Italia (Received May 3, 1960).

The simplest reactions of associated production in proton-proton collisions are investigated with the aid of two simple models, which consider as relevant only the contribution due to the exchange of one intermediate π meson or K meson, respectively. The values of the total cross sections predicted by these models are calculated at various energies up to 3.5 Gev of the incident proton in the lab system. These cross sections are related to the experimental cross sections for simpler processes, namely associated production by pions (first model) and K^+-nucleon scattering (second model). Both models give the same order of magnitude for the cross sections for all reactions (10^{-2} mb at lower energies, 10^{-1} mb at higher energies), except for Σ^0 production, where the results predicted by the two models differ by a factor of 10. Some of the calculated values are affected by large errors, due to the uncertainty of the experimental data which are used.

ANTIPROTON-PROTON CROSS SECTIONS AT 1.0, 1.25, AND 2.0 Bev. Rafael Armenteros,* Charles A. Coombes,† Bruce Cork, Glen R. Lambertson, and W. A. Wenzel, Lawrence Radiation Laboratory, University of California, Berkeley, California (Received April 29, 1960).

The interaction of 1.0-, 1.25-, and 2.0-Bev antiprotons with protons has been studied with the aid of a 4π solid-angle scintillation-counter detector system. The measured total cross sections at the above energies are 100, 89, and 80 mb, respectively. At each energy, the charge-exchange cross section is approximately 5 mb. The total elastic cross sections are 33, 28, and 25 mb, respectively, at the three energies. The angular distribution of elastic scattering has been fitted with a simple optical-model calculation.

*On leave of absence from Conseil Nucléaire de Recherche Scientifique and Laboratoire de Physique, Ecole Polytechnique, Paris, France.
†Present address: University of Idaho, Pocatello, Idaho.

BRANCHING RATIO OF THE ELECTRONIC MODE OF POSITIVE PION DECAY. H. L. Anderson, T. Fujii, R. H. Miller,* and L. Tau,† The Enrico Fermi Institute for Nuclear Studies, The University of Chicago, Chicago, Illinois (Received May 13, 1960).

A new measurement of the branching ratio $(\pi^+ \to e^+ + \nu)/(\pi^+ \to \mu^+ + \nu)$ has been completed. A double-focussing magnetic spectrometer was used to observe the spectra of electrons emitted in π decay and in μ decay. The scintillation pulses from the pion and its decay electron were recorded on a travelling-wave oscilloscope. Timing and pulse-height measurements were used to distinguish good events from accidentals. The total number of π-e events recorded in this experiment was 1346, of which 6% were accidentals and 5% were π - μ - e contamination. The branching ratio obtained from an analysis of the data over the π - e and μ - e distributions and corrected to include all decay electrons was $(1.21 \pm 0.07) \times 10^{-4}$. This is close to the result expected for a universal V-A interaction. Kinoshita's calculation, taking into account radiative effects, gave 1.23×10^{-4}. Our data also gave for the mean life of π decay $\tau_\pi = (25.6 \pm 0.8) \times 10^{-9}$ second.

*Now at Yerkes Observatory, the University of Chicago, Chicago, Illinois.
†Now at Institute of Physics, University of Rome, Rome, Italy.

HYPERBOLIC MOTION IN CURVED SPACE-TIME. W. Rindler, Department of Mathematics, Cornell University, Ithaca, New York (Received May 2, 1960).

The differential equations of motion for a test particle moving with uniform acceleration in a

curved space-time are proposed. They are obtained by generalizing the differential-geometric characteristics of a rectangular hyperbola in Minkowski space-time. The problem is proposed, though not solved, of deriving these equations of motion from the field equations of general relativity. However, it is suggested that they also hold independently of general relativity in cosmological space-times based on the Robertson-Walker metric. The equations are solved in detail for the particular case of de Sitter space-time, which is relevant to the steady state theory. It is found, inter alia, that in this space-time a particle moving by radially uniform acceleration ultimately moves with constant relative velocity through the substratum; that there is a critical first fundamental particle (galaxy) on its line of motion which it will never overtake; that, in turn, a light signal emitted at or after a certain critical time will not catch up with the accelerating particle; and that, if a particle with a given available acceleration α passes beyond a certain proper distance (the α horizon) it can no longer return to its place of origin. Possible applications to intergalactic rocketry are examined.

MESON-MESON SCATTERING TERM AND LOW-ENERGY PION-NUCLEON SCATTERING. Masao Sugawara and Akira Kanazawa,* Physics Department, Purdue University, Lafayette, Indiana (Received May 4, 1960).

The modified Chew-Low integral equation for the pion-nucleon P-wave scattering amplitudes was derived by the present authors using the Chew-Low-Wick formalism and assuming a general static interaction Hamiltonian plus the meson-meson scattering term. Essentially the same result is shown to follow from dispersion relations in the no-nucleon-recoil approximation if we assume that the almost-forward elastic scattering amplitude becomes a finite real number at large incident pion energy. If we further presume that the meson-meson scattering term alone is responsible for this asymptotic behavior, we can show that the extra term to be introduced into the Chew-Low integral equation is just the zero-energy limit of the corresponding term, which was energy dependent in our previous derivation. The modified effective-range expansion of the P-wave phase shift is compared with the data. The S-wave integral equations are also given; they are formally much simpler than those obtained previously in the static model calculation.

*On leave of absence from Hokkaido University, Sapporo, Japan.

STRONG INTERACTIONS AND A MODEL FOR HYPERONS. I. Goldberg, Department of Physics, University of Michigan, Ann Arbor, Michigan and Leon F. Landovitz, Brookhaven National Laboratory, Upton, New York (Received April 14, 1960).

Using a four-dimensional approach, the couplings of the strongly interacting particles are restricted in a simple way which is not inconsistent with experiment. This leads to the consideration of a Goldhaber-type model. The gross properties of the hyperons are calculated in the intermediate-coupling approximation for this model.